

CAAP Quarterly Report

[03/30/2024]

Project Name: *Multi-Compound Green Corrosion Inhibitor for Gas Pipeline: Synthesis, Optimization, and Evaluation*

Contract Number: 693JK32350004CAAP

Prime University: *Arizona State University*

Prepared By: *Xuandong Lu, Qihang Xu, Saumya Dimple Mehta, Kapil Chandra Akula, Mohammadjavad Kazemi, Sai Niranjana, Essam Abdel Rahman (PhD students), Dr. Yongming Liu (PI), Dr. Shuguang Deng (Co-PI), Dr. Tekle Fida (Co-PI)*

Reporting Period: [12/2023 – 3/2024]

Project Activities for Reporting Period:

Task 1. Design and Synthesis of Multi-compound Green Inhibitors

During this reporting period, we have made significant progress in Task 1, focusing on the design and synthesis of green inhibitors and establishing test methods for evaluating the performance of the inhibitors. The key activities are outlined below:

- 1.1: Synthesis of Pectin from Orange Peels
 - Executed a thorough study to optimize the extraction and synthesis of pectin from orange peels, recognized as a potential eco-friendly inhibitor.
 - Investigated methods for the functionalization of pectin to enhance its corrosion inhibition performance.
- 1.2: Development of Two Corrosion Test Methods and Preliminary Results on Pectin Inhibitor
 - Formulated a weight loss experimental protocol for testing the corrosion inhibition of bio-inhibitors.
 - Established an electrochemical corrosion test experimental protocol for assessing the corrosion inhibition of bio-inhibitors.
- 1.3: Synthesis of Chitosan-Derived Inhibitor
 - Initiated a study on the extraction and synthesis of Chitin and Chitosan from shrimp shells, identified as a promising eco-friendly inhibitor.

Task 2. Simulation-based inhibitor optimization in Gas Gathering and Transportation Pipelines

During this reporting period, we have made significant progress in Task 2, focusing on establishing the neural network framework for more efficient prediction on the flow regime. The key activities are outlined below:

- 1.1: Mapping between wall shear stress and roughness
 - Constructed a roughness model in ANSYS Fluent accurately producing original data for network training.
 - Built and trained the model of Fourier Neural Operator that estimated wall shear stress

- highly fitting to theoretical values.
- 1.2: Multi-fidelity data integration
 - Constructed a pipe model and study the flow regime under different fidelities.
 - Applied convolutional neural network to achieve high accuracy in predicting key fluid dynamics parameters.

A detailed report for the above two tasks is included in the appendix. The presentation file for the quarterly report with technical advisory panel (TAP) members and PHMSA program managers is also included in the appendix.

Project Financial Activities Incurred during the Reporting Period:

For Task 1, we supported 1 RA at ASU

For Task 2, we supported 2 RA at ASU

Project Activities with Cost Share Partners:

Discussions with technical advisory panel members for suggestions on team research activities.

Project Activities with External Partners:

Regular discussions with the technical advisory panel and several individual meetings with advisory members.

Potential Project Risks:

Nothing to report.

Future Project Work:

For Task 1:

- Continue with the functionalization and modification of pectin
- Initiate the synthesis and modification of chitosan-derived inhibitors
- Set up baseline corrosion data for inhibitors based on chemicals
- Carry out evaluations of pectin and chitosan inhibitors
- Construct a comprehensive database for all inhibitors, including both chemical and green variants
- Finalize the candidates of renewable feedstock to be investigated in this project.
- Summarize the industry standards regarding the compatibility and safety of green inhibitors.

For Tasks 2:

- Improve the applied numerical model to be more efficient by introducing local boundary condition near the roughness segment
- Introduce random roughness models to improve the generalization of WSS prediction networks
- Extend the multi-fidelity prediction model to include simulations of more complex

geometries and flow conditions

- Further refine the multi-fidelity model's architecture and training processes to enhance its predictive accuracy and computational efficiency

Potential Impacts to Pipeline Safety:

The proposed study will mitigate internal corrosion risk by developing environmentally friendly inhibitors and optimizing their performance.

Appendix 1
Technical progress description for task 1

Task 1. Design and Synthesis of Green Inhibitors

Background and Objectives in the Current Quarter

Background:

In the initial phase of our project, we embarked on an extensive journey to design and synthesize eco-friendly corrosion inhibitors. This marked a crucial step in our quest for sustainable solutions to the widespread issue of pipeline corrosion. Our efforts were characterized by a strategic focus on harnessing renewable resources. We specifically concentrated on the innovative use of citrus peels and began preliminary studies into shrimp shells as potential sources for creating environmentally friendly inhibitors. The primary objectives of these endeavors were twofold: to reduce the environmental impact associated with traditional petroleum-based inhibitors and to maximize the use of waste materials. This approach aligns with the global urgency for sustainable development.

Informed by a thorough review of the literature, our research efforts shed light on potential avenues for identifying effective green corrosion inhibitors. This foundational work was enhanced by the creation of specialized experimental protocols designed to facilitate the transformation of these renewable resources into powerful agents for corrosion mitigation. Furthermore, our adherence to industry standards and practices demonstrated our commitment to ensuring the compatibility and safety of our synthesized inhibitors, in line with existing infrastructure materials and operational norms. The culmination of these preliminary efforts resulted in the successful synthesis of pectin from orange peels and the development of a comprehensive framework for corrosion testing methodologies, thereby laying a solid groundwork for future stages of our project.

Objectives in the Previous Quarter

As we progressed into the previous quarter, our goals were carefully designed to encourage ongoing innovation and improvement in the field of green corrosion inhibitors. At the heart of our efforts was the goal to refine the extraction and synthesis processes of pectin from orange peels, building on the promising results of our initial experiments. This concentrated endeavor was aimed at validating the effectiveness and feasibility of pectin as a key element in our corrosion mitigation strategy, marking a new era in the use of green inhibitors. We also explored methods to enhance the efficiency of pectin's corrosion inhibition on metal surfaces. Concurrently, we expanded our research scope by initiating the synthesis of a chitosan-derived inhibitor from shrimp shells, thereby broadening our range of green inhibitors. This expansion not only demonstrated our commitment to investigating sustainable material sources but also underscored our dedication to environmental stewardship by valorizing waste materials for ecological and industrial benefits.

Alongside the synthesis and optimization efforts, our project was dedicated to the meticulous development and refinement of corrosion testing methodologies. The creation of weight loss and electrochemical experimental protocols was envisioned to establish a comprehensive and robust framework for assessing the corrosion inhibition effectiveness of our bio-derived inhibitors. This all-encompassing approach harmonized the innovative synthesis of new green inhibitors with the essential requirement for dependable testing methodologies. Through these unified and multidisciplinary efforts, our project aimed to make significant contributions to the field of sustainable corrosion protection, thereby addressing the industrial necessities of safety and efficiency within an eco-friendly framework.

Task 1.1: Synthesizing Pectin from Orange Peels

- Undertaking an In-Depth Study to Optimize the Extraction and Synthesis of Pectin from

Orange Peels: A Promising Green Inhibitor”

Pectin, a naturally occurring polysaccharide, is predominantly found in the cell walls of terrestrial plants, especially within the rinds of fruits. It serves as a remarkable example of nature’s intricate design. This biopolymer primarily consists of repeating units of galacturonic acid, which amalgamate to form a flexible and complexly branched polymer structure. The structure of pectin is characterized by the presence of carboxyl (-COOH) and hydroxyl (-OH) functional groups. These groups bestow upon pectin its distinctive water solubility and the unique capability to form gels under specific conditions. These attributes render pectin invaluable in the food industry, where it plays a crucial role in the production of jams and jellies. Moreover, pectin’s potential extends beyond culinary applications to more technologically advanced uses, such as inhibiting corrosion in steel. This highlights the versatility and potential of this remarkable biopolymer.

The use of pectin as a “green” corrosion inhibitor signifies a transformative shift towards environmentally sustainable practices in the realm of metal protection. Traditional methods of corrosion inhibition, which frequently depend on synthetic chemicals, are increasingly under examination due to their potential environmental and health impacts. Pectin, owing to its biodegradable nature and minimal toxicity, emerges as an eco-friendly alternative. This aligns with the escalating demand for sustainable solutions in the industry, demonstrating that pectin’s potential extends far beyond its culinary applications. This shift not only addresses environmental concerns but also paves the way for innovative, green technologies in corrosion prevention.

When applied to steel surfaces, pectin utilizes its carboxyl and hydroxyl groups to establish a protective barrier against corrosive agents. This barrier is thought to adhere to the metal surface, thereby inhibiting the electrochemical processes that result in corrosion. Pectin’s effectiveness in this role is credited to its capacity to form stable complexes with metal ions. This characteristic significantly diminishes the metal’s vulnerability to oxidative reactions, which are responsible for rusting. Moreover, the gel-forming ability of pectin may play a pivotal role in shielding the metal surface from corrosive environments. This not only prolongs the lifespan of steel structures but also mitigates the adverse environmental impacts associated with traditional corrosion inhibitors. This highlights the potential of pectin as a sustainable solution in corrosion prevention.

The emerging field of research exploring the use of pectin as a corrosion inhibitor for steel and other metals carries significant potential. This extends beyond the safeguarding of vital infrastructure to advancing the fields of green chemistry and sustainable materials science. As researchers delve deeper into understanding the mechanisms behind pectin’s inhibitory effects, the scope for its wider application becomes increasingly evident. This ongoing exploration opens up the possibility for the development of more effective and environmentally friendly strategies for corrosion prevention. This underscores the potential of pectin to contribute to a more sustainable future.

In the first segment of **Task 1.1**, we build upon our preliminary efforts to extract pectin from orange peels, as depicted in Figure 1 from the previous quarter. Our focus is on intensively optimizing the process involved in the extraction and synthesis of pectin.

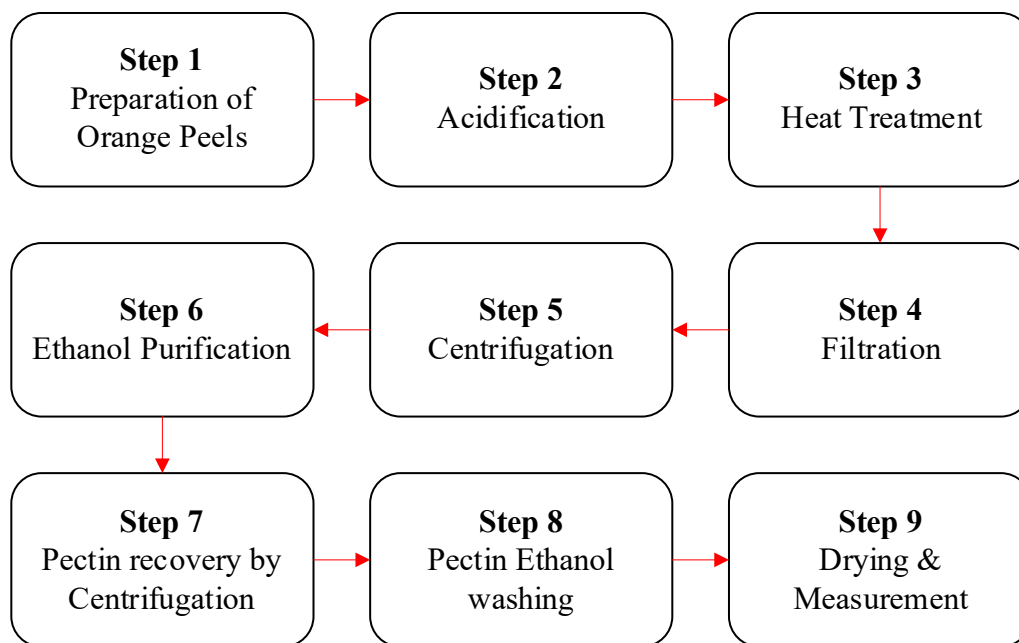


Figure 1. Main steps for pectin extraction from citrus peels

The extraction of pectin from citrus peels entails a sequence of meticulous steps designed to isolate this valuable polysaccharide with accuracy and efficiency. This process employs a blend of chemical and physical techniques to facilitate the breakdown of cell walls, leading to the subsequent release of pectin. In the following sections, we provide a detailed, step-by-step description of the approach we adopted in our experiment.

1. Preparation of Orange Peels

- The orange peels were initially subjected to cutting to enhance the surface area available for extraction.
- Subsequent washing was performed to remove any adhering dirt or contaminants.
- Post-washing, the peels were thoroughly dried to eliminate excess moisture.

2. Measurement and Acidification

- A precise weight of 45 grams of the prepared orange peel was measured to ensure consistency.
- These were then placed into a container with 500 ml of deionized water.
- Hydrochloric acid (HCl) was added dropwise to the solution to achieve a pH level of 1.0, facilitating the disruption of pectin-containing cell walls within the peels.

3. Heat Treatment

- The acidified mixture was transferred to a beaker and subjected to heat treatment.
- A constant temperature of 90°C was maintained for 3 hours, with continuous stirring to promote uniform heating and prevent charring.

4. Filtration

- After heating, the hot solution was filtered to remove the solid remnants of the orange peels.
- The filtration utilized a fine-mesh material capable of allowing the passage of the pectin-rich solution while retaining the bulky solids.

5. Centrifugation

- The filtered solution was subjected to centrifugation at a speed of 4000 rpm for 15 minutes.
- This process aided in the separation of the pectin from other soluble impurities.

6. Ethanol Purification

- Post-centrifugation, the pectin was precipitated by adding 98% Ethanol.
- The addition of ethanol precipitated the pectin, enabling its separation from the aqueous phase.

7. Centrifugation

- The Ethanol precipitated solution was subjected to another centrifugation at a speed of 4000 rpm for 15 minutes.

8. Pectin Washing

- Post-centrifugation, the pectin was washed with 60% Ethanol.

9. Drying

- The precipitated pectin was carefully collected and spread evenly on a drying tray.
- This was placed in an oven preheated to 60°C for 4 hours, ensuring thorough drying without degradation.
- The dried pectin was weighed to quantify the yield.

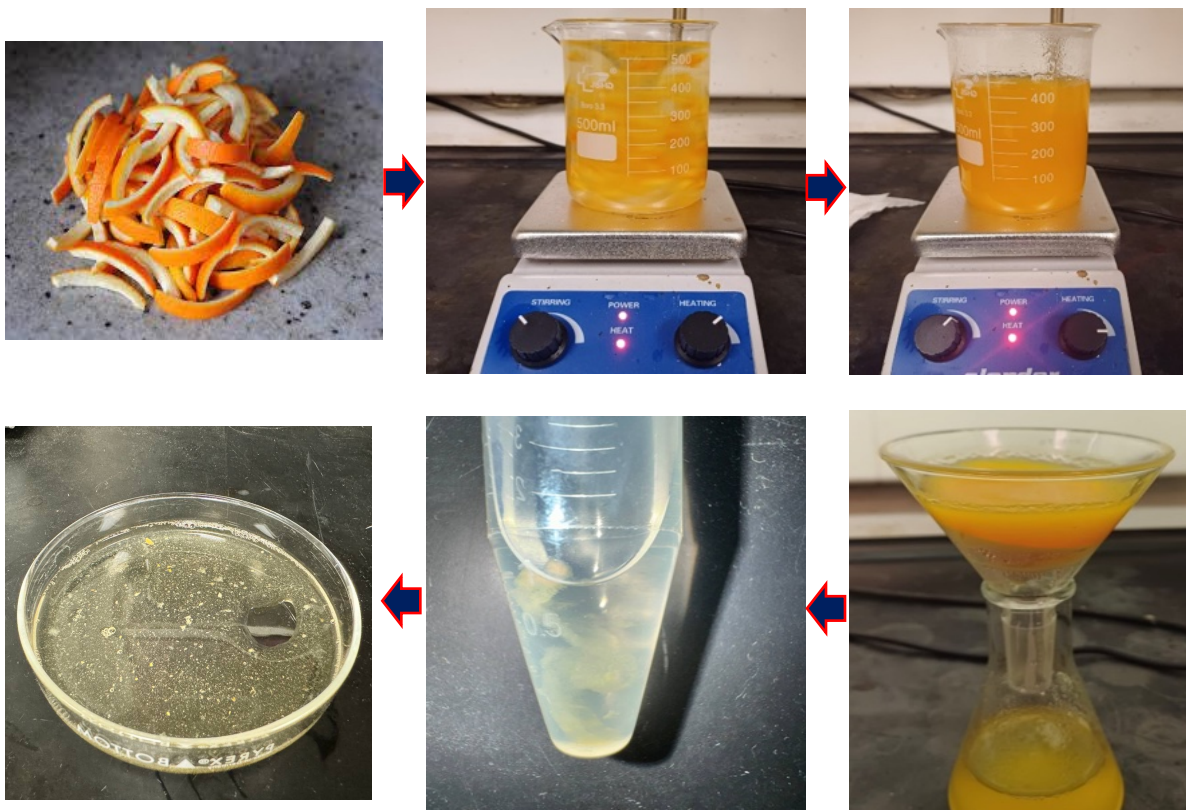


Figure 2. Illustration of the conducted pectin extraction process

Figure 2 provides a visual representation of the extraction process we conducted. Throughout this methodology, we paid meticulous attention to preserving the integrity of the pectin structure. The process was designed with dual objectives in mind: to maximize the yield and to ensure that the extracted pectin met the standards necessary for its use in the food, pharmaceutical, and industrial sectors. This comprehensive protocol underscores the careful and deliberate approach required to extract high-quality pectin from citrus peels.

- Exploring Methods for Pectin Functionalization to Enhance Its Corrosion Inhibition Performance

In the second phase of **Task 1.1**, our team undertook a comprehensive literature review to comprehend the mechanism for enhancing the corrosion inhibition functionality of extracted pectin. The literature review on methods for surface modification of pectin using amine groups unveiled a sophisticated chemical strategy aimed at augmenting the adhesive capabilities of pectin through the incorporation of amine functionalities. Pectin, a naturally occurring polysaccharide, is distinguished by the presence of carboxyl groups (-COOH) along its molecular backbone. Under standard conditions, these groups exhibit limited reactivity, posing a challenge for their direct application in surface modification endeavors. However, the use of 1-Ethyl-3-(3-dimethylaminopropyl) carbodiimide (EDC) and N-hydroxysuccinimide (NHS) as activating agents transforms these dormant carboxyl groups into reactive intermediaries. These intermediaries are capable of forming stable amide bonds with primary amines, thereby enhancing the functionality of pectin as a corrosion inhibitor.

The activation process, facilitated by EDC and NHS, plays a crucial role in the chemical modification of pectin. EDC, a water-soluble carbodiimide, operates efficiently within the pH range of 4.0 to 6.0. It serves as a carboxyl-activating agent that encourages the coupling of primary amines, leading to the formation of amide bonds. Simultaneously, NHS selectively targets the carboxyl groups of pectin, forming an NHS ester intermediate that exhibits high reactivity towards primary amines. This selective activation ensures that other functional groups within the pectin molecule remain untouched, thereby preserving the inherent properties of the polysaccharide while boosting its reactivity. This strategic approach enhances the functionality of pectin without compromising its natural characteristics.

The strategic activation of pectin's carboxyl groups results in a notable improvement in its adhesive properties. This process facilitates the formation of covalent bonds between pectin and molecules or surfaces bearing amine groups, fostering a more robust and enduring adhesion compared to methods that rely on physical adsorption or weak chemical interactions. This enhanced adhesion is vital for applications that demand a strong, stable, and long-lasting attachment to a variety of substrates, including metals, polymers, and biological materials. The capability of the modified pectin to form robust covalent linkages translates into superior adhesion strength, increased resistance to mechanical stresses, and enhanced long-term stability of pectin-based coatings or modifications. This highlights the potential of pectin as a versatile and sustainable material in various applications.

In conclusion, the literature highlights a promising strategy for modifying pectin through the incorporation of amine groups, capitalizing on the chemical activation of carboxyl groups using EDC and NHS. This method not only boosts the reactivity of pectin but also broadens its applicability in a range of surface modification applications. This signifies progress in the development of eco-friendly inhibitors and the engineering of biomaterials with improved adhesive properties. This underscores the potential of pectin as a versatile and sustainable material in various applications.

Task 1.2: Establishing Two Corrosion Test Methods and Preliminary Results on Pectin Inhibitor

- Formulation of a Weight Loss Experimental Protocol for Testing Bio-Inhibitors' Corrosion Inhibition and Preliminary Results on Pectin's Efficacy

The corrosion testing utilized A36 steel sheets, which are characterized by an unpolished (mill) finish, hot-rolled, and conform to ASTM A36 standards. These steel sheets, with a thickness of 0.06 inches, were fashioned into test coupons measuring 2.0 cm by 1.0 cm. A corrosive medium was formulated using 1M hydrochloric acid (HCl), derived from 37 percent analytical reagent (AR) grade HCl. This solution was designed to mimic harsh corrosion conditions. To evaluate the corrosion resistance of the steel coupons under various conditions, three distinct mediums were prepared. This approach allowed for a comprehensive assessment of the material's performance under different corrosive environments.

Medium 1 (Control): Pure 1M HCl solution, serving as the control to assess the effect of the corrosive medium on unprotected A36 steel.

Medium 2 (Pectin Mixed): A solution consisting of 0.2 g of pectin dissolved in 100 ml of water, mixed with pure 1M HCl. This medium aimed to investigate the influence of pectin presence in the corrosive media on steel corrosion.

Medium 3 (Pectin Pre-coating): Steel specimens were initially immersed in a pectin solution (0.4 g of pectin in 100 ml of water) to form a dip-coating layer of pectin gel on the surface. Subsequently, these pre-coated coupons were immersed in 1M HCl solution. This setup was designed to measure the effect of pectin pre-coating on corrosion protection.

The differences in weight loss across the three mediums were analyzed to assess the efficacy of pectin in mitigating corrosion on A36 steel.

Test Procedure

For each test, the corresponding steel coupons were fully submerged in a 500 ml glass beaker filled with one of the prepared test solutions. The experiments were carried out over a span of 24 hours at a regulated temperature of 25 °C. To minimize the impact of oxygen and maintain uniform conditions, the beakers were situated in a fume hood. Prior to immersion, each steel coupon was precisely weighed to establish its initial mass. After the 24-hour exposure period, the coupons were removed from their respective solutions. Any corrosion products that formed during the test were eliminated by thoroughly scrubbing each coupon under running water using a bristle brush. Following the cleaning process, the coupons were dried in acetone to eliminate any remaining moisture. They were then reweighed to ascertain the final mass. This meticulous process ensures the accuracy of the corrosion testing results.

The principal evaluation metric for this experiment was the weight loss of the steel coupons, determined by subtracting the final mass from the initial mass of each coupon. This calculation offered a quantitative evaluation of the corrosion rate experienced by the steel in each medium. This allowed for a comparison of the protective effects of pectin against corrosion, whether mixed in the solution or applied as a pre-coating. **Table 1** presents the average result of the weight loss test under each condition, along with the efficiency of the pectin coating and pectin dispersion compared to the control sample. This data provides a comprehensive overview of the performance

of pectin as a corrosion inhibitor under different conditions.

The inhibitor efficiency is a measure of how effectively a corrosion inhibitor decreases the corrosion rate when added in small concentrations to an environment. It can be calculated using the following equation:

$$\text{Inhibitor Efficiency (\%)} = 100 \times (\text{CR}_{\text{uninhibited}} - \text{CR}_{\text{inhibited}}) / \text{CR}_{\text{uninhibited}}$$

where:

CR_{uninhibited} is the corrosion rate in the absence of the inhibitor.

CR_{inhibited} is the corrosion rate in the presence of the inhibitor.

Table 1. Summary of corrosion weight loss test results

	Medium 1 (Control)	Medium 2 (Pectin Mixed)	Medium 3 (Pectin Pre- coating)
Ave. weight before corrosion (g)	7.451	7.837	6.288
Ave. weight after corrosion (g)	7.363	7.804	6.238
Weight loss (g)	0.088	0.033	0.055
Corrosion percentage	1.18%	0.42%	0.79%
Corrosion inhibitor efficiency	-	62.5%	33%

- Formulation of an Electrochemical Corrosion Test Protocol for Evaluating the Corrosion Inhibition Performance of Bio-Inhibitors

The second phase of **Task 1.2** outlines the experimental protocol we developed to evaluate the corrosion inhibition performance of bio-inhibitors through electrochemical corrosion tests.

Experimental Setup

The foundation of our experimental protocol was established with the use of a Versastat 4 potentiostat. Initially, we encountered a firmware limitation (version 450) that disabled the corrosion module. To overcome this challenge, we upgraded the firmware to version 500 and employed a specialized corrosion cell. This cell includes a Saturated Calomel Electrode (SCE) as the reference electrode and a graphite electrode serving as the counter electrode. We designated carbon steel specimens, both cylindrical and flat, as working electrodes. This configuration is crucial for the subsequent electrochemical tests: Electrochemical Impedance Spectroscopy (EIS) and Tafel polarization tests. These tests aim to shed light on the protective capabilities of green inhibitors.

Electrochemical Corrosion Tests

Tafel Extrapolation

The Tafel extrapolation method, a fundamental component of our protocol, offers a quantitative evaluation of corrosion rates and mechanisms. This destructive test involves plotting the current density against the potential, which reveals crucial parameters such as the corrosion

potential (E_{corr}) corrosion current density (i_{corr}), Tafel slopes (β_a and β_c), and ultimately, the corrosion rate (CR). These metrics are essential for comprehending the anodic and cathodic reactions that drive corrosion in the presence of bio-inhibitors. This method provides a comprehensive understanding of the corrosion process and the effectiveness of green inhibitors.

Electrochemical Impedance Spectroscopy (EIS)

Electrochemical Impedance Spectroscopy (EIS) provides a nondestructive method for examining corrosion kinetics and mechanisms across a wide frequency range. By utilizing sinusoidal AC perturbation and Fast Fourier Transform (FFT) analysis, this technique generates plots of impedance magnitude versus frequency, phase angle, and Nyquist plots.

Key results include the determination of equivalent circuit parameters, double-layer capacitance (C_{dl}), and corrosion rates (CR). The EIS data, when further analyzed through adsorption isotherms, illuminates the dynamics of surface interactions of bio-inhibitors. This analysis distinguishes between physisorption and chemisorption mechanisms, providing a comprehensive understanding of the corrosion process and the effectiveness of bio-inhibitors.

Objective

The primary objectives of this experimental protocol are to:

- Investigate the mechanisms and kinetics of corrosion in the presence of bio-inhibitors.
- Evaluate the efficacy of bio-inhibitors in inhibiting corrosion.
- Develop models to understand the behavior of corrosion and the interaction of inhibitors.
- Optimize strategies for corrosion protection based on empirical data.
- Draw conclusions based on the findings.

Through the execution of this carefully crafted experimental protocol, we aim to deepen our understanding of bio-inhibitors in corrosion prevention. The suite of electrochemical tests, including Tafel extrapolation and EIS, offers a thorough assessment of the inhibitors' performance. This forms the basis for optimizing eco-friendly corrosion protection solutions. Our approach not only contributes to the field of corrosion science but also aligns with the global trend towards sustainable and environmentally conscious corrosion mitigation strategies. Figure 3 illustrates the assembled test setup for the Electrochemical Corrosion Test, providing a visual representation of our experimental setup.

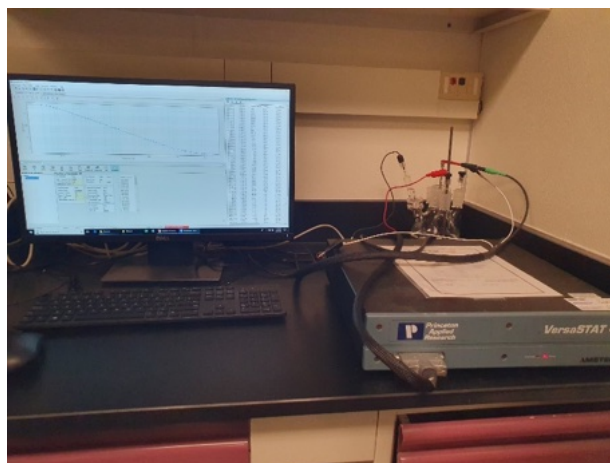


Figure 3. Electrochemical corrosion test setup

- **Task 1.3: Synthesizing Chitosan-Derived Inhibitor**
 - Initial Study on the Extraction and Synthesis of Chitin and Chitosan from Shrimp Shells: A Promising Green Inhibitor

The protocol outlined below was meticulously developed and adhered to for the extraction of Chitosan from shrimp shells. Shrimp shells were procured from a local fish market and underwent a thorough purification process. The chemical reagents used in this process were of pure grade, guaranteeing the integrity of the extraction process. The methodological approach we developed, characterized by its systematic steps of deproteinization, demineralization, and deacetylation, effectively facilitates the extraction of chitosan from shrimp shells.

Step 1: Preparation of Shrimp Shell Powder

Initially, the shrimp shells were thoroughly cleaned and then dried in an oven at 65 °C for a period of 4 days until they were completely dehydrated. Following this, the dried shells were ground into a fine powder. This powder was stored in a sealed container and preserved in a freezer to maintain the inherent properties of the shells.

Step 2: Deproteinization

For the deproteinization step, 15 g of the shrimp shell powder was subjected to an alkaline treatment, where it was mixed with 75 ml of a 1 M sodium hydroxide solution (maintaining a 1:5 w/v ratio). This mixture was then heated and stirred at a temperature of 30°C for a duration of 20 hours. After the alkaline treatment, the mixture was filtered and thoroughly rinsed with distilled water until it reached a neutral pH of 7. Once a neutral pH was achieved, the powder was dried in an oven overnight at a temperature of 60 °C. This prepared the powder for the next step, which is demineralization.

Step 3: Demineralization

During the demineralization phase, the deproteinized shrimp shell powder underwent treatment with a 2% hydrochloric acid solution, maintaining a solid-to-solvent ratio of 1:5 (w/v). This mixture was continuously stirred at a temperature of 30°C for a duration of 16 hours. After the treatment, the residue was filtered and then thoroughly rinsed with distilled water until it reached a neutral pH. The resulting material was dried overnight in an oven, resulting in the production of chitin. This process ensures the effective extraction of chitin from shrimp shells.

Step 4: Deacetylation

The process of deacetylation involves the treatment of chitin with a potent 50% (w/v) sodium hydroxide solution. This treatment facilitates the removal of acetyl groups, thereby transforming chitin into chitosan. The reaction is carried out at a temperature of 60 °C, maintaining a solid-to-solvent ratio of 1:10 (w/v) over a duration of 20 hours. Upon completion of the deacetylation process, the resultant material is thoroughly rinsed with water until it reaches a neutral pH level. Subsequently, the material is dried in an oven for a period of 15 hours at a temperature of 60 °C. The final product obtained from this process is chitosan.

Figure 4 provides a visual representation of the procedure employed for the extraction of chitosan from shrimp shells.

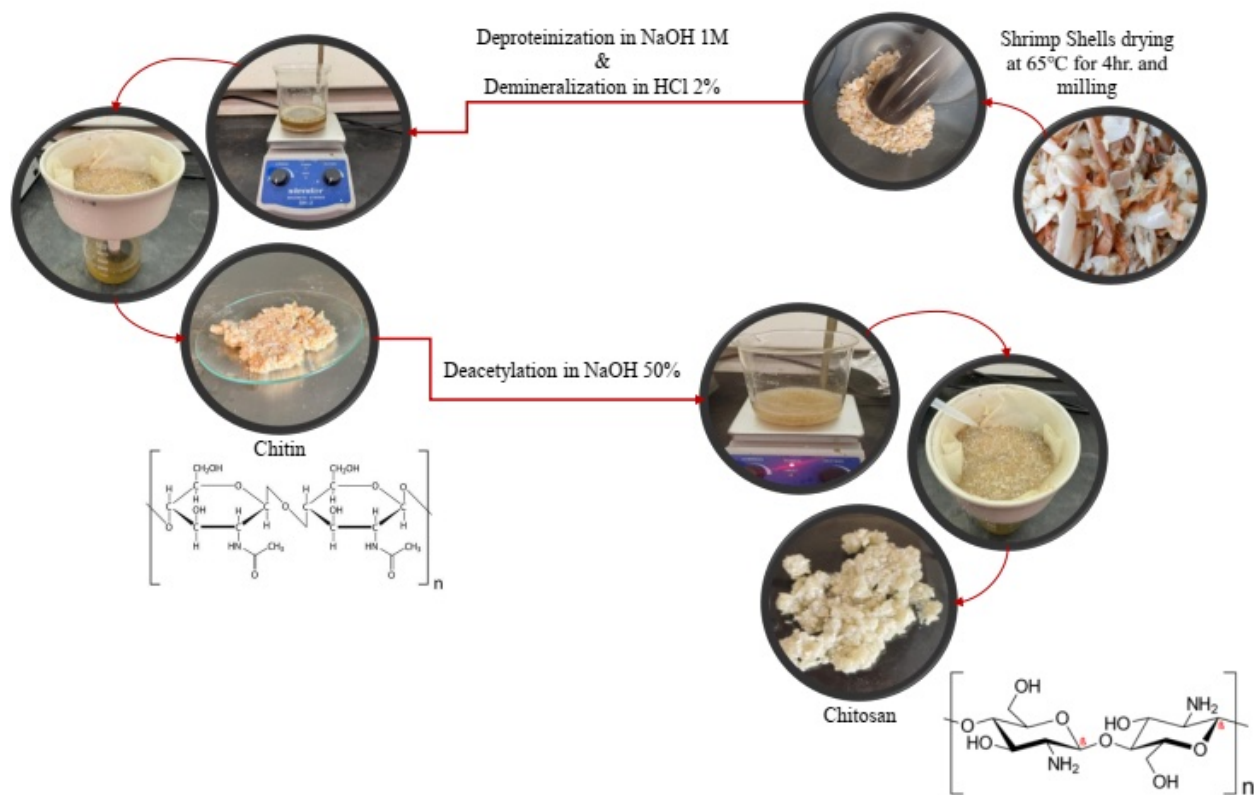


Figure 4. Chitosan extraction process from shrimp shells

To summarize, throughout this reporting period, our team has made substantial advancements in the design and synthesis of eco-friendly corrosion inhibitors. Noteworthy achievements encompass the successful refinement of the pectin extraction process from orange peels, the preliminary synthesis of chitosan from shrimp shells, and the establishment of stringent corrosion testing methodologies. These endeavors have established a robust groundwork for upcoming tasks, which include additional functionalization of pectin, enhancement of chitosan-based inhibitors, and an all-encompassing assessment of their corrosion prevention capabilities.

Related Comments and Response of Task 1

Question 1:

In the corrosion test, A36 steel sheets were selected for testing. But I think it is necessary to verify the surface condition of hot-rolled A36 steel sheets present the surface condition of pipe grade steel used for pipeline construction, because the surface condition is the most important factor affecting the effectiveness of inhibitors.

Response to Question 1:

We acknowledge that the surface morphology of metal plays a crucial role in its corrosion behavior and the performance of corrosion inhibitors. It should be highlighted that the selection of hot-rolled A36 steel sheets was based on a comprehensive review of standards and literature relevant to the production and utilization of gas pipeline materials. Despite our efforts to obtain materials that closely mimic the components of the pipes used in the field, we faced limitations in acquiring pipe-grade steel. Therefore, the hot-rolled A36 steel is chosen, which is widely recognized for its application in gas pipeline construction and features an unpolished surface similar to that of operational pipelines.

We made this choice to ensure that our investigation maintains a high degree of relevance to real-world applications, given the constraints. Our primary objective at this stage is to identify the most effective green corrosion inhibitors for a material that closely approximates the surface condition of pipeline steel. We intend to apply the most promising inhibitors to actual pipeline sections in subsequent phases of our research, thus directly addressing the practical implications of our findings.

We believe that this approach strikes a balance between the ideal conditions for testing and the practical limitations we face, ensuring that our results are both reliable and applicable to the field. We remain committed to further refining our methodology as more resources become available, with the ultimate goal of enhancing the integrity and longevity of pipeline infrastructure.

Question 2:

You used 1M HCl as the corrosion test medium for the corrosion screening test. It will be helpful to include the tests with the corrosion medium that represents the pipeline operating environment, at least include some validation tests to verify the behavior of the corrosion inhibitors in the 1M HCl corrosion test represents that in the field so that the selection of corrosion inhibitors will be applicable for future field implementation.

Response to Question 2:

We agree that selecting a test medium that closely resembles the conditions encountered by pipelines in service is crucial to ensuring the validity and applicability of our findings to field implementations.

1M HCl is chosen as the corrosion medium based on a thorough review of existing literature that frequently identifies it as a standard for preliminary corrosion testing of steel, including pipeline applications. This choice was motivated by the need to establish a baseline for corrosion inhibitor performance under well-understood and reproducible conditions.

Although we understand that this approach has its limitations in comprehensively capturing the complexity of pipeline environments, we intend to expand our testing by incorporating additional corrosive media that more accurately simulate real-world operational conditions. Specifically, we aim to include tests involving CO₂-saturated medium and gasoline to cover a wider range of practical applications.

These subsequent tests are designed to validate the effectiveness of the identified corrosion inhibitors in a variety of conditions, ensuring their relevance and applicability to actual pipeline operations. By comparing the performance of inhibitors across different media, we aim to identify those with the broadest and most effective protection range, thereby facilitating their future field implementation.

Appendix 2
Technical progress description for task 2

Task 2. Simulation-based Inhibitor Implementation Optimization in Gas Gathering and Transportation Pipelines

1. Introduction

1.1 Background

In the realm of gas pipeline systems, the integrity of pipelines is paramount, not only for the efficiency of transportation but also for environmental and safety reasons. The application of corrosion inhibitor in the realm of gas pipeline systems efficiently saves the financial consumption for pipeline maintenance and reduced safety hazards. Most existing research and scholarly works tend to collect short-term corrosion data and thus is more concerned about the damage of fierce flow to local corrosion inhibitors, e.g. the pipe elbow and mutation of the wall shape.

At more general locations of the pipeline, the inhibitor protective film would be in a sustained weakening by the flow and will gradually loss adhesion over time. Therefore, the inhibitor film attached on the pipe wall needs to supplement at certain intervals. However, Characteristics of many new types of inhibitors are not clear, resulting in the difficulty to specify the plan for the utilization of corrosion inhibitors. Overly frequent supplementation of inhibitors will cause unnecessary resource waste. On the contrary, failure to timely fill the failed protective film may lead to irreversible damage to the pipe wall and the reduction in its service life. This research aims to investigate the flow-induced degradation of the inhibitor film.

Flow-induced degradation is primarily attributed to the fluid dynamics within the pipeline, where multiple phases of matter - gases, liquids, and occasionally solid particles - interact with the inner walls. Compare to the static liquid, this interaction more likely to trigger the disintegration of the protective inhibitor layer, leaving the metal surface vulnerable to corrosive agents.

Wall shear stress (WSS) serves as a key metric for assessing the impact of multiphase flow on corrosion inhibitor films. Figure 1 depicts how the flow of gas or liquid exerts WSS, adversely affecting the protective efficacy of inhibitor films on pipeline walls. This type of stress generates a velocity gradient within the inhibitor layer, which exerts a long-term effect on the degradation of the corrosion inhibitors, although the flow under low velocity hardly has the ability to tear the film layer instantly. Such degradation leaves the pipeline wall in higher risk and vulnerable to corrosive environments if the supplementation of the inhibitor film does not come timely. Therefore, the stability of the corrosion inhibitor film under fluid flow is evaluated using WSS as a pivotal reference, highlighting the critical relationship between flow dynamics and the integrity of corrosion protection.

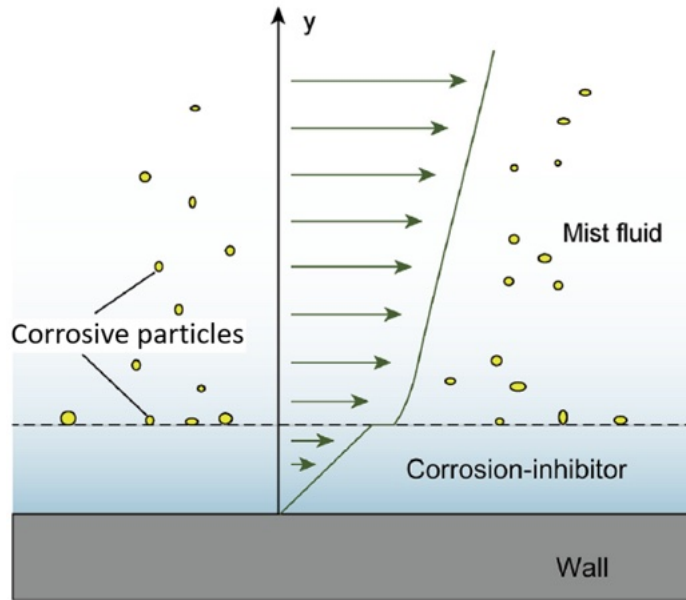


Figure 1: Effect of multiphase flow on the corrosion inhibitor film and the distribution of velocity gradients within the film.

Wall roughness is another key metric to evaluate the stability of the inhibitor film. Traditional CFD modelling is inclined to build the flow boundary in the pipe as the smooth wall, which is quite different from its real condition. Figure 2 shows the maximum WSS when the wall roughness is considered at the flow boundary. The undulating wall depicted in Figure 2(b), (c) and (d) significantly increases the computational WSS, thus increasing the failure probability of the protective film. Therefore, incorporating wall roughness into the research of flow-induced degradation of the inhibitor film is beneficial for promoting mechanical simulation and failure prediction of pipelines closer to the reality.

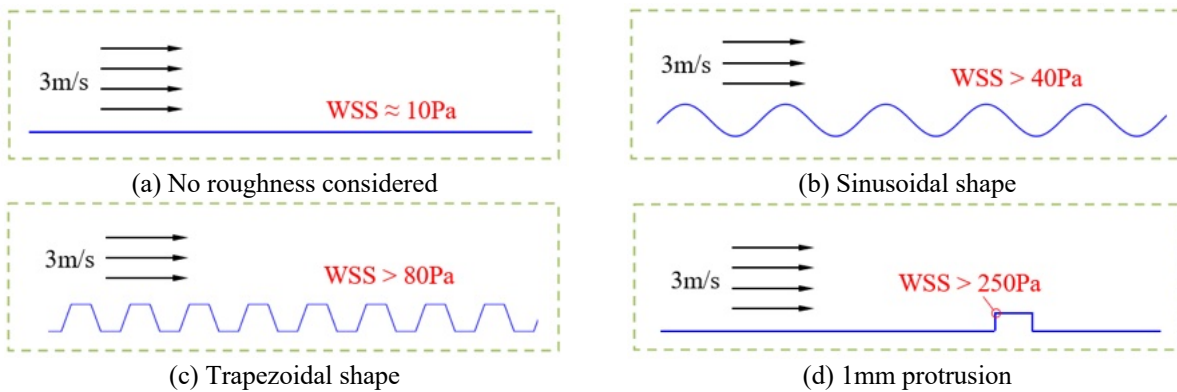


Figure 2: Maximum wall shear stress under typical roughness.

WSS is presented in variable types of distributions with different forms of wall roughness. In this process, a difficulty emerges that high-fidelity (HF) meshing is required for many possible cases of roughness to ensure the modelling precision, which leads to significant cost of computational resource and time. Providing a large amount of HF data is not usually feasible with limited computation resource and time. In most CFD cases, HF data, known for its high accuracy but typically limited in quantity, provides detailed insights into the simulated phenomena. In contrast,

LF data, which is more abundant but less precise, covers a broader range of conditions with varying levels of detail. In this consideration, a potential approach is to perform the neural network that learn the features in the integrate of HF data and LF data. To leverage the strengths of both data types, a balance can be achieved between detail and coverage, so that less requirement will be asked for HF data and the efficiency of producing original baseline can be improved.

The primary focus of this paper is to build a network to efficiently predict WSS from the shape of wall roughness, which can contribute to later research of specifying the degradation of corrosion inhibitors in the flow. Figure 3 depicts the flowchart of predicting degradation of the inhibitor film.

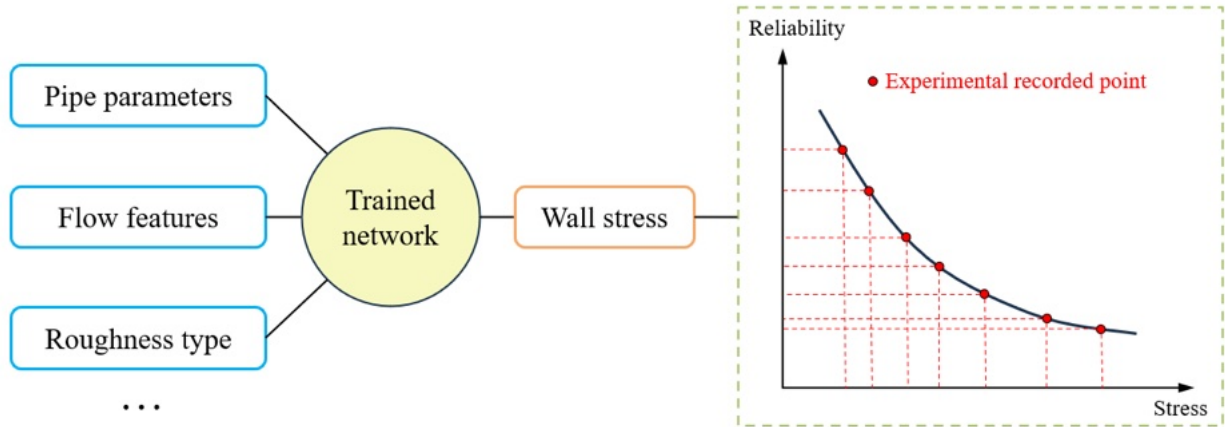


Figure 3: Flowchart of predicting degradation of the inhibitor film.

We also aim to validate the hypothesis that integrating both High-Fidelity (HF) and Low-Fidelity (LF) data into a single training model could enhance the model's predictive accuracy and reduce the overall simulation time. Achieving high accuracy and efficiency in these predictions is crucial for validating the simulation model's applicability to real-world scenarios and for ensuring that the produced original data is reliable for usage.

The outcomes of this study are expected to contribute significantly to the development of more effective strategies for pipeline protection, enhancing the longevity and safety of these critical components in the energy infrastructure.

1.2 Objectives

The main objective of this research is to employ the Fourier Neural Operator (FNO) for the direct mapping between the shape of wall roughness and analytical WSS currently considered as the main factor affecting the stability of inhibitor film.

A key aim is to create a series of HF data related to wall roughness and analytical WSS. This study will construct a suitable roughness model that can reflect the practical near-wall flow regime.

The research also seeks to develop a multi-fidelity data integration model that integrates both HF and LF data into a single training model, which is potential to enhance the model's predictive performance with less requirement for HF data.

Additionally, the study aims to train a convolutional neural network (CNN) model based on the integrated dataset, achieving high accuracy in predicting key fluid dynamics parameters to ensure that the reliability of produced data.

By achieving these objectives, the simulation project aspired not only to contribute to improving the longevity and safety of pipelines but also to demonstrate a scalable and efficient model for conducting simulations that traditionally require significant computational efforts from engineering design and analysis to research and development in fluid mechanics.

2. Methodology

2.1 WSS Prediction

In establishing the neural network for a fast prediction of WSS, the application of CFD models is indispensable as the source of training the network. A series of 2-D pipe segments is analyzed to produce the dataset under different shapes of wall roughness. Then, the framework of FNO is applied to build the mapping between WSS and wall roughness.

2.1.1 Roughness model

Before extending to more general random roughness, a series of regular shape of roughness was employed to originally test the ability of FNO. At this point, the 2-D wall roughness was first considered in sinusoidal shape and defined by the amplitude and the frequency of the sinusoidal function. Figure 4 depicts several applied shapes of wall roughness.

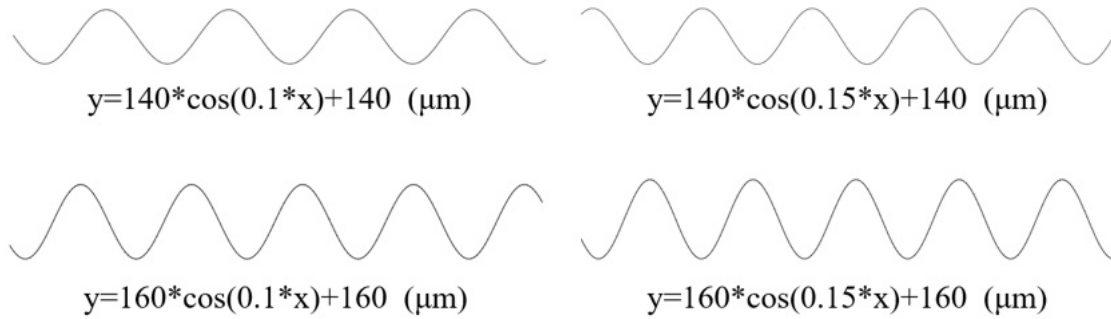


Figure 4: Example of shapes of roughness with sinusoidal expressions.

2.1.2 Meshing and solution

The ANSYS software is employed for physical modeling and mesh generation in pipeline systems. Figure 5 provides an example of a 2D pipe with wall roughness. Wall roughness is set at a 0.05m-length boundary with the remaining part of being totally smooth. This configuration ensures the fully developed flow field in the enough length of the pipe and save the time for meshing without the fully-distributed roughness.

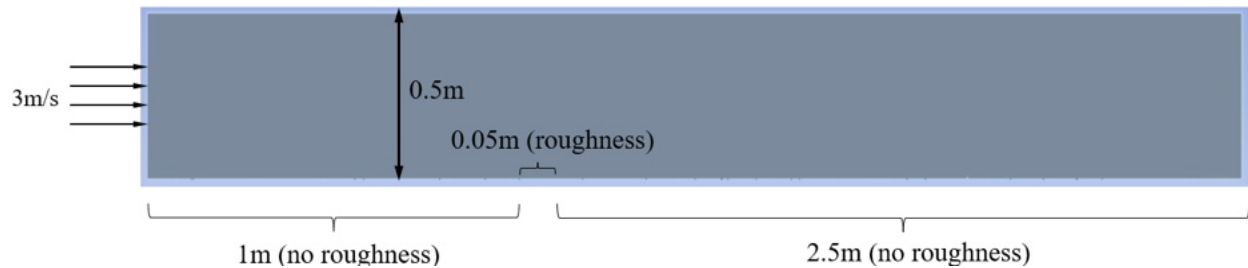


Figure 5: Example of the 2D pipe with wall roughness.

In our simulation of the near-wall flow regime, a variety of parameters are meticulously considered to produce precise baseline data for network training. These parameters are categorized into two CFD steps: meshing and solution. Figure 6 shows meshing details to illustrate the critical parameters

- **Meshing Properties:**

- **General size:** The general size of grids affects the accuracy of the flow field in the upper area. In the currently considered low-speed steady flow, the flow solution can still converge even when the general size is in a relatively large value (up to 5 mm).
- **Refinement size:** The refinement size is crucial to computational accuracy at near-wall locations. It is better to set it as fine as possible, but time consuming of meshing is almost in exponential growth with the decreasing refinement size. In this study, the refinement size of 30 μm is used.
- **Inflation layer:** Grid inflation is beneficial to improve the gradient computation of near-wall flow regime. For the studied case without large gradient changes, two

inflation layer is enough to optimize the quality of meshing.

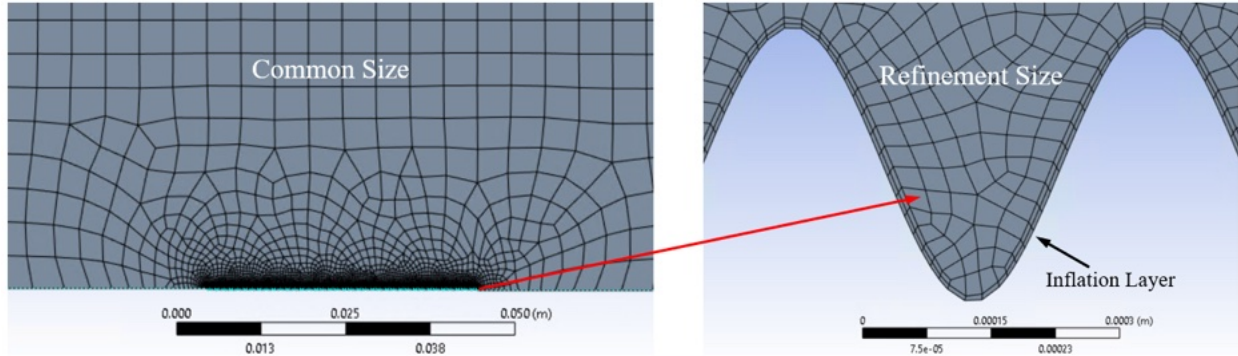


Figure 6: Details of meshing for the roughness model.

• **Solution Properties:**

- **Viscous model:** The viscous model is related to the exchange of momentum, energy, and concentration among fluid media, which influence flow dynamics and computational WSS results. The $k-\omega$ model is used to simulate flow viscous.
- **Boundary condition:** This term usually contains a velocity inlet and a pressure outlet for better control of the initial flow rate, so does this study. The upper boundary of the simulation pipe is set to symmetry, which provides double width for the flow that makes the flow field far way from the roughness more stable.
- **Solution method:** The “Coupled” method is applied that solve momentum and continuity equations in a tightly coupled manner. This can accelerate the convergence of the solution significantly.

2.1.3 Training data

A naïve neural network needs to be trained by a series of data under different scenarios. For existing studies, input data contains two coordinates of 2-D grid nodes, of which the analytical WSS is set into output data. Figure 7 gives the illustration for data extraction from a certain case. Flow enters the roughness segment from smooth segment before $x=0$ cause sudden change in WSS, which stabilizes at around $x=0.02$. For this reason, data of a 0.02-length segment between $x=0.02$ and $x=0.04$ is set as training, while the last 0.01-length segment is set as testing. Specifically, each training or testing set contains the data at 200 continuous nodes, in which original values of x -coordinate and WSS are used, while the derivative of y over x ($y'=\Delta y/\Delta x$) replace y values to form the dataset. This modification for y considers the more important impact of relative roughness height on WSS.

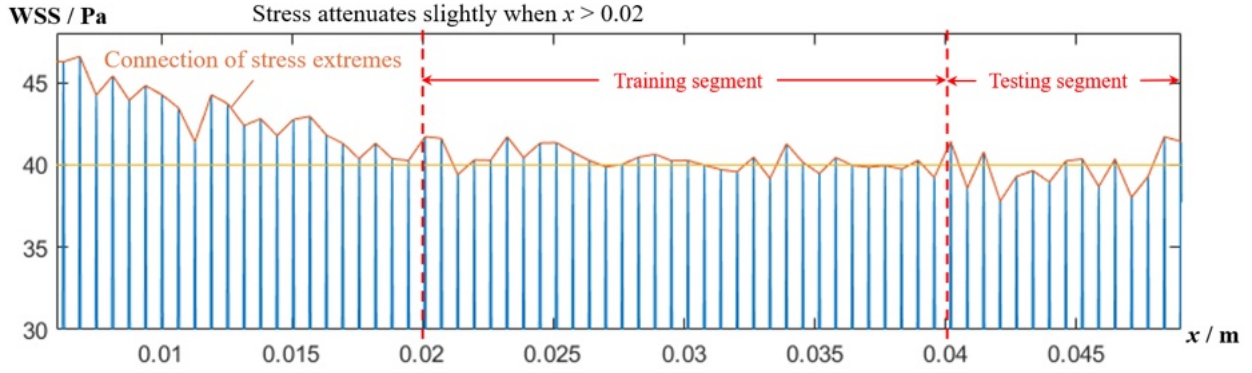


Figure 7: Details of meshing for the roughness model.

2.1.4 Neural network

The advanced FNO is applied to build the mapping between the shape of roughness and WSS. This work is first proposed in (Z. Li, N. Kovachki, K. Azizzadenesheli, B. Liu, K. Bhattacharya, A. Stuart, A.J.a.p.a. Anandkumar, Fourier neural operator for parametric partial differential equations, (2020). As shown in Figure 8, it is formulated as an iterative architecture $v_0 \rightarrow v_1 \rightarrow \dots \rightarrow v_T$ where v_j for $j = 0, 1, \dots, T - 1$ is a sequence of functions. The inputs x and y' is first lifted to a higher dimensional representation $v_0(x, y') = P(x, y')$ by the local transformation P which is usually parameterized by a shallow fully-connected neural network. Then several iterations of updates $v_t \rightarrow v_{t+1}$ are applied. As a result, the output $u(x, y') = Q[v_T(x, y')]$ is the projection of v_T by the local transformation from the space- v to the space- u . In each iteration, the update $v_t \rightarrow v_{t+1}$ is defined as the composition of a non-local integral operator K and a local, nonlinear activation function σ . FNO has the ability to find critical feature of series in the frequency domain, which is potential to map the shape of roughness into analytical WSS.

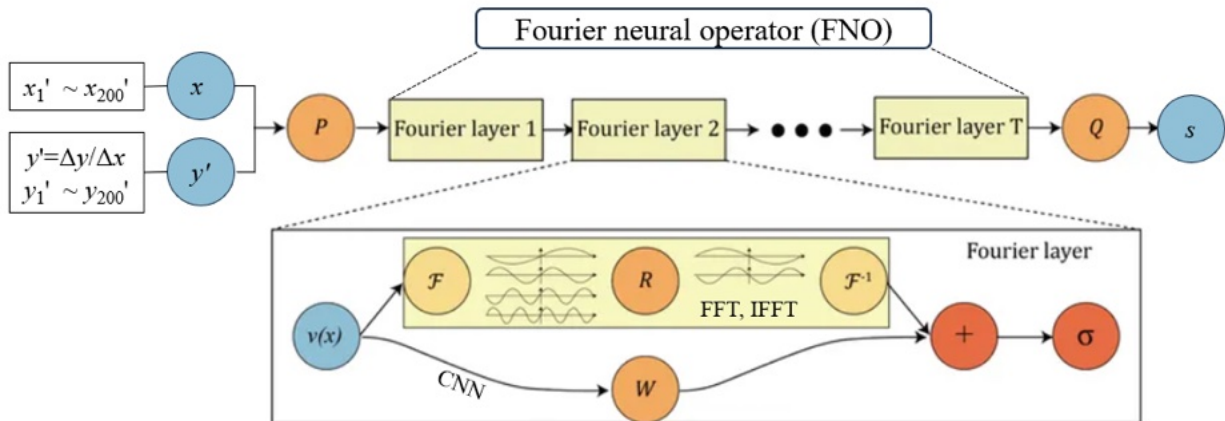


Figure 8: The framework of FNO.

Constructing as comparison, a traditional fully-connected neural network (FCNN) is shown in Figure 9. Other settings of network training are listed in Table 1, which shows similar number of parameter included in FNO and FCNN.

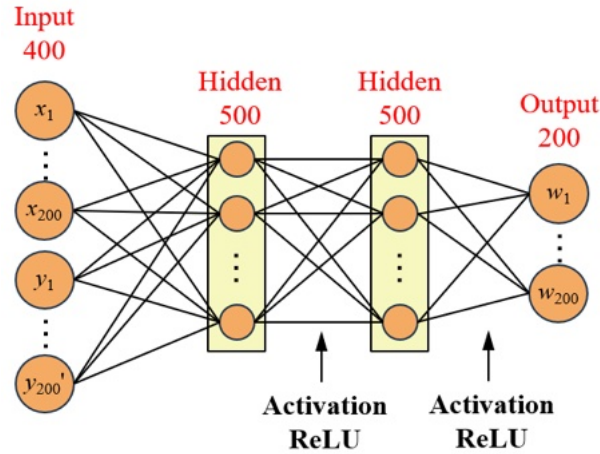


Figure 9: The framework of FCNN as comparison.

Table 1. Settings of FNO and FCNN.

Settings	FNO	FCNN
Parameters number	549569	551200
Epoch number	600	600
Average time consumption in each epoch (s)	2.23	0.77
Batch size	1	1
Original learning rate	0.001	0.001
Learning rate decay	0.5 per 50 steps	0.5 per 50 steps

2.1.5 Results of network operation

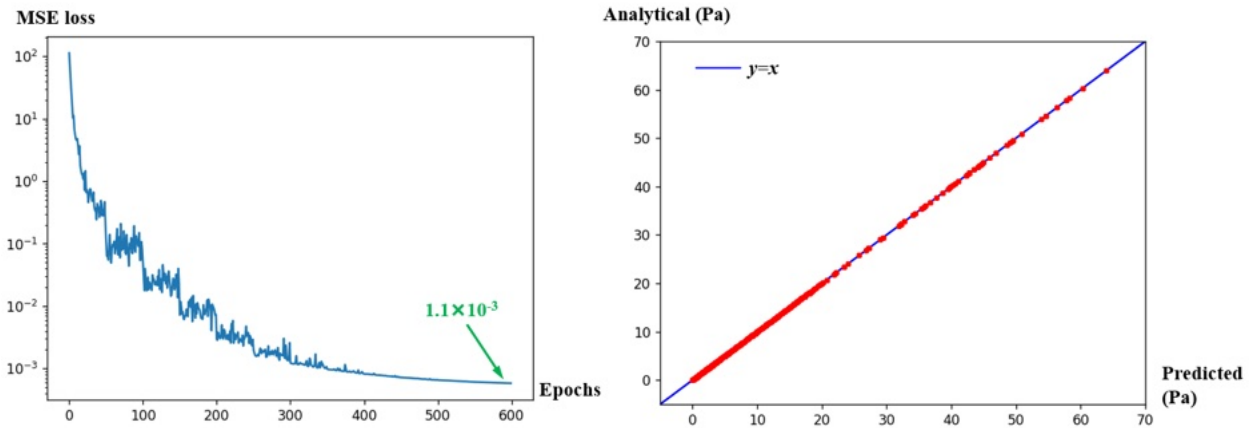


Figure 10: Illustration of the training process and testing results of FNO.

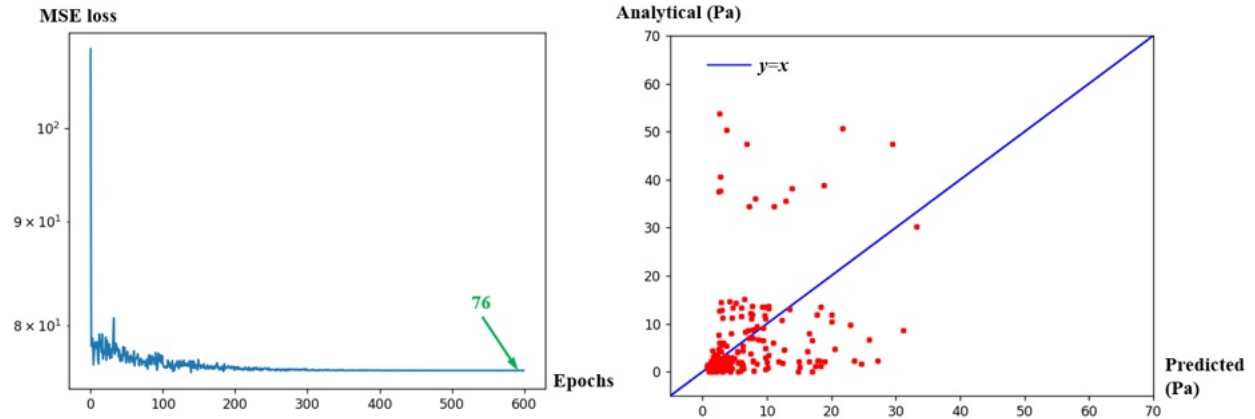


Figure 11: Illustration of the training process and testing results of FCNN.

The training process and testing results of FNO in Figure 10 indicate a good performance of FNO in predict WSS. In comparison, those in Figure 11 show that FCNN cannot effectively identify the sinusoidal shapes of wall roughness so that the training loss stagnates at the value of 76. As expected from the training results, WSS is mostly wrongly predicted in the testing set. The better performance of FNO can be illustrated by its process of the fast Fourier transform and the inverse fast Fourier transform involved. As mentioned, data in each node is continuously selected to form the training set and testing set, and thus the selected series have uncertain start nodes and end nodes. Figure 12 presents the illustration for this condition. At this point, FCNN will identify this kind of data as irregular, since the values with the same order in each set are totally different. On contrast, FNO has the ability to catch the law of roughness changes. Transformed into the frequency domain, critical features of all shapes of roughness become clear.

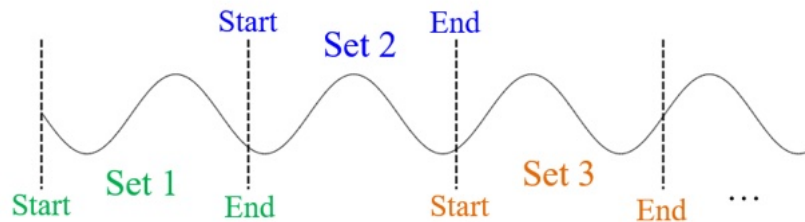


Figure 12: Illustration for the uncertain start nodes and end nodes of each dataset.

2.2 Multi-fidelity data integration

The simulation in this section embarked on a comprehensive exploration to ascertain the feasibility and effectiveness of employing a multi-fidelity data training approach. CNN is utilized for the prediction of CFD results within a specific segment of the pipe.

2.2.1 Pipe model

Different from the roughness model, the pipe conditions for production of the multi-fidelity data were specifically designed to create a realistic and controlled environment for assessing the effectiveness of the multi-Fidelity data training approach using Convolutional Neural Networks (CNN). The simulation focused on a simplified model of a pipe section, representing a common scenario in fluid dynamics studies. The conditions within the pipe were meticulously set to ensure that the simulations could accurately reflect the behavior of fluids under various operational parameters. Key aspects of the pipe conditions include:

- **Geometry and dimensions:** The pipe section modeled in the simulation was chosen to reflect typical dimensions and geometry encountered in practical applications. This included considerations for the pipe's diameter, length, and wall thickness, ensuring that the simulated environment closely mimics real-world conditions.
- **Boundary conditions:** The simulation established specific boundary conditions at the pipe's inlet and outlet, as well as along its walls. At the inlet, a uniform velocity profile was applied to simulate the flow entering the pipe section. The outlet was modeled to allow the fluid to exit without causing significant backpressure or flow disturbances. The walls of the pipe were treated to reflect no-slip conditions, a fundamental assumption in fluid dynamics that dictates zero velocity at the boundary, simulating the interaction between the fluid and solid surfaces.
- **Flow characteristics:** The flow within the pipe was assumed to be incompressible and laminar, typical of many fluid transport scenarios in pipes at moderate velocities and viscosities. This assumption simplifies the analysis while still providing valuable insights into the flow behavior and the effectiveness of the CNN model in predicting fluid dynamics under these conditions.

Figure 13 show the 2-D pipe model to study multi-fidelity data integration, where u and v are flow rates in two directions. By setting these pipe conditions, the simulation aimed to create a controlled yet realistic environment for evaluating the CNN model's ability to predict fluid dynamics accurately.

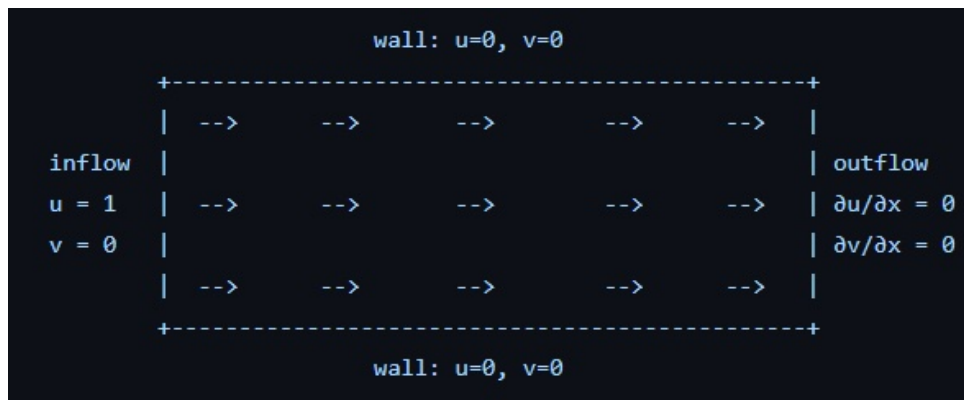


Figure 13: Pipe model for the study of multi-fidelity data integration.

The careful consideration of geometry, boundary conditions, flow characteristics, and material properties ensured that the simulation results would be relevant and applicable to real-world engineering problems, enhancing the validity and applicability of the multi-fidelity data training approach in fluid dynamics simulations.

2.2.2 Pipe simulation

Figure 14 provides the streamline distribution of the HF flow and the LF flow. The HF data, characterized by a dense mesh and intricate flow vectors, provides a detailed representation of the fluid's velocity and pressure gradients, yielding a comprehensive analysis of fluid behavior within the system. Conversely, the LF data employs a sparser mesh with less detail in the flow vector representation, offering a broader, more generalized view of the flow dynamics. This contrast underscores the LF data's utility in scenarios where computational efficiency is prioritized, whereas the HF data is indispensable for applications requiring high precision and detail in the simulation results.

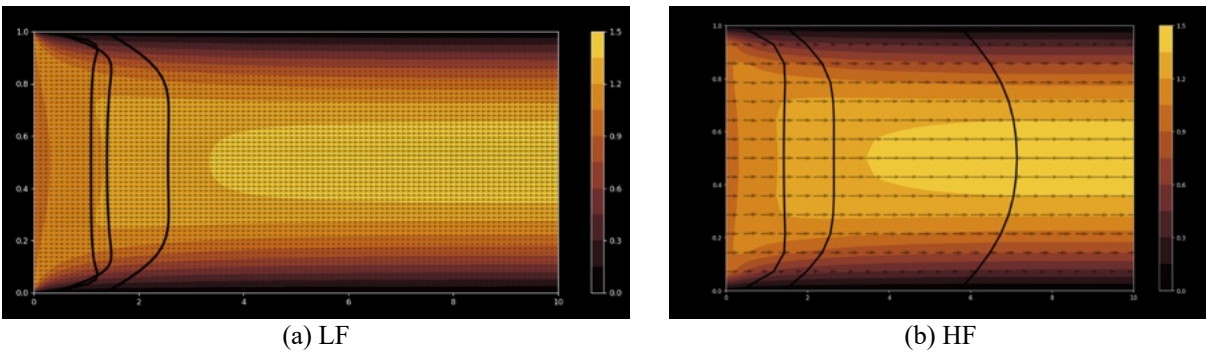


Figure 14: Streamline distribution under different fidelity.

2.2.3 CNN prediction

A CNN model, designed to accommodate multi-fidelity data, is trained using these datasets. The architecture of the CNN is carefully tailored to extract and learn from the patterns inherent in both HF and LF data, enabling it to predict the fluid dynamics with a high degree of accuracy.

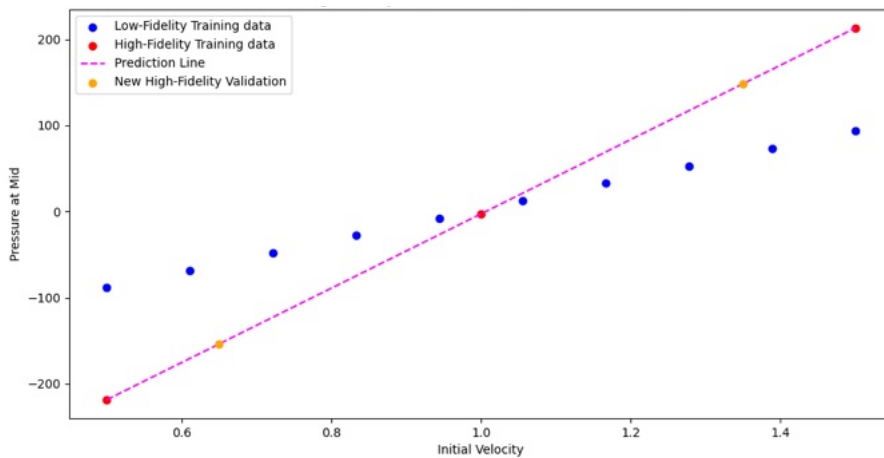


Figure 15: Results of predicted pressure under different fidelities.

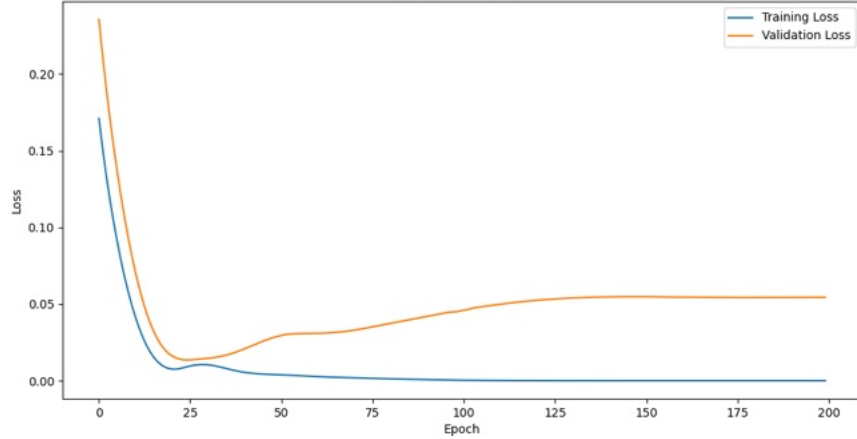


Figure 16: Training loss over epochs.

Results from the simulations confirm the model's efficacy, as they successfully predict pressure values across various velocities, aligning closely with the trends observed in the HF data. This validation demonstrates the potential of the multi-Fidelity training approach to enhance prediction accuracy while optimizing computational resource utilization. The methodology not only achieves high precision in simulation outcomes but also presents a scalable solution that can reduce the computational burden associated with traditional fluid dynamics simulations.

3. Future Direction

In the part of WSS prediction, the application of FNO, while shows excellent performance in reflecting the real WSS distribution, fail in estimation with the shape of wall roughness that never occur in the training set, let alone considerable possible shapes like rectangle, triangle and even the random field. To address these challenges, we propose the integration of the Chebyshev data sampling from a Gaussian random that comes from the idea of operator training. This strategy is potential to produce many representative shapes of wall roughness that are expected to fit by enough sinusoidal functions. Figure 17 illustrates the random roughness shape and the meshing detail.



Figure 17: Random roughness shape (left) and its meshing detail (right).

The integration with Transformer is another necessity to improve the generalization of WSS prediction. Figure 18 shows the model architecture of Transformer. The core idea of Transformer is the attention mechanism, which calculates the interrelationships among all entries in a sequence. This relationship is considered to reflect the correlation and importance among different entries to some extent. Therefore, the relationship can be used to adjust the weight of each entry and further obtain new features for it, which not only contains the entry itself but also the relationships with other entries, making it a more global representation. Corresponding to the roughness mode, it is

evident that the WSS results of each grid point are related with the roughness height of its surrounding points. This relationship is expected to be clarified in the subsequent established Transformer model.

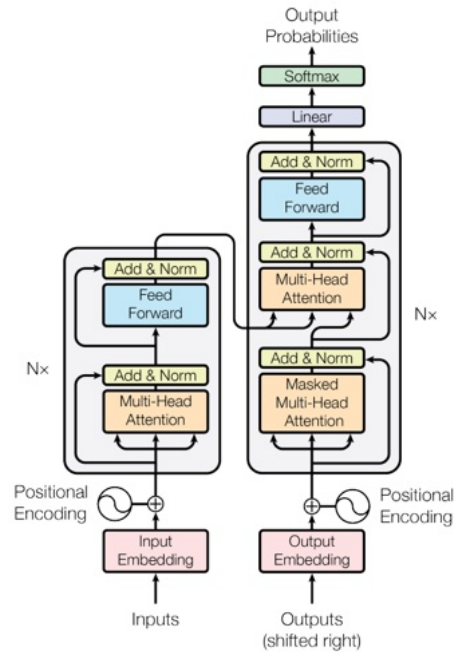
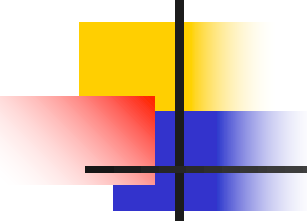


Figure 18: Model architecture of Transformer.

For the part of multi-fidelity data integration, its scope will be extended to include simulations of more complex geometries and flow conditions, such as those encountered in slightly turbulent flows and multi-phase simulations. These advancements are intended to test the robustness and versatility of the CNN model under a wider array of conditions, further validating its applicability to real-world fluid dynamics challenges. Additionally, efforts will be directed towards refining the model's architecture and training processes to enhance its predictive accuracy and computational efficiency.

Appendix 3
Presentation files for quarterly TAP meeting

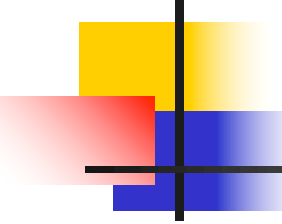


Multi-compound green corrosion inhibitor for gas pipeline: synthesis, optimization, and evaluation

Investigators: Yongming Liu (PI), Shuguang Deng, Tekle Fida

Student: Sai Niranjan, Mohammadjavad Kazemi, Essam Abdel Rahman,
Qihang Xu, Saumya, Xuandong Lu, Dimple Mehta,
Kapil Chandra Akula

March 21, 2024



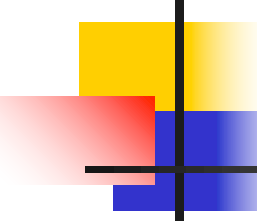
Summary of progress

- **Experimental task**

- Synthesized pectin from orange peels and explore methods to functionalize pectin
- Synthesized chitosan-derived inhibitors
- Established two corrosion test methods

- **Simulation/AI/ML task**

- Develop the inhibitor degradation mechanism model with wall shear stress (WSS)
- Develop Fourier operator network to predict WSS
- Develop a multi-fidelity model using a convolutional neural network for computational efficiency

A decorative graphic consisting of overlapping yellow, red, and blue squares with a black crosshair.

Task 1: Design and Synthesis of Green Inhibitors

Progress made in Q2

- Synthesized pectin from orange peels
- Explored methods to functionalize pectin
- Synthesized chitosan-derived inhibitors
- Established two corrosion test methods
- Contacted industry advisory board members regarding green inhibitors (Dow, Baker Hughes)
- Initial results on pectin inhibitor

Task 1: Design and Synthesis of Green Inhibitors

Task 1.2: Synthesis and Characterization of Green Inhibitors from Renewable Feedstock

Plant or Source	Active Constituent	Solvent & Extraction Method	Metal to Protect	Corrosive Environment	Corrosion Inhibition Efficiency (%)	Inhibitor Concentration
Citrus peel	Pectin	HCl and ethanol	Mild steel	1M HCl	94.2 at 45 °C	2 g L ⁻¹
Shrimps shell waste	Chitosan	NaOH	Carbon steel	1M HCl	88.5 at 25 °C	10 ⁻⁵ M
Plantago ovata	Polysaccharide (galacturonic acid)	Water	A1020 carbon steel	1M HCl	94.4 at 45 °C	1 g L ⁻¹
Rhododendron schlippenbachii	Polyphenolic compounds	Methanol	Low carbon steel	1M H ₂ SO ₄	94.2 at 30 °C	600 ppm

Examples of bio-based corrosion inhibitors to be investigated in this project

Task 1: Design and Synthesis of Green Inhibitors

Pectin

- Pectin is a naturally occurring polysaccharide found in the cell walls of plants, especially fruits.
- Its structure is composed of repeating units of galacturonic acid, forming a flexible and branched polymer.
- Pectin contains carboxyl (-COOH) and hydroxyl (-OH) groups, making it water-soluble and capable of forming gels. As a "green" corrosion inhibitor, pectin can be used to protect metals from rusting in eco-friendly ways.

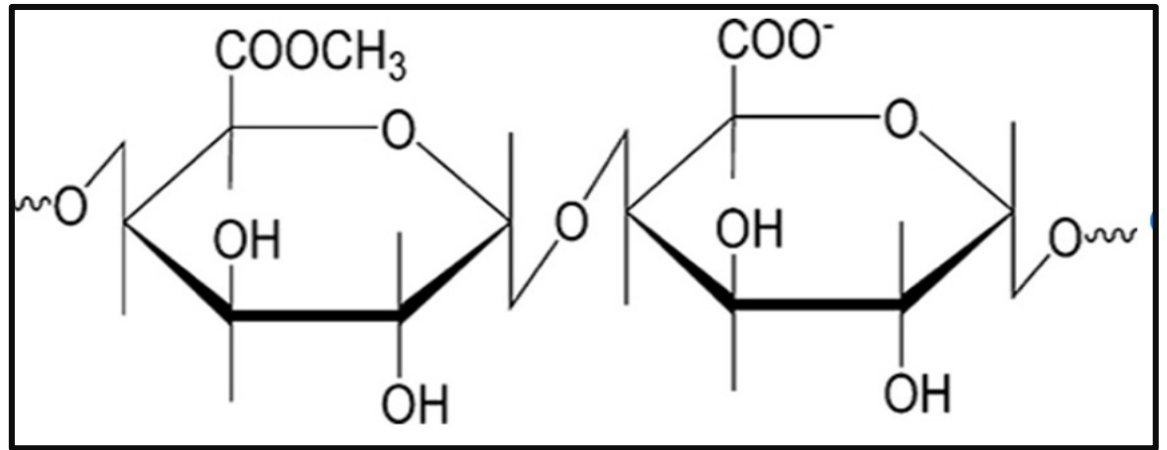


Illustration of the molecular formula of pectin.

Task 1: Design and Synthesis of Green Inhibitors

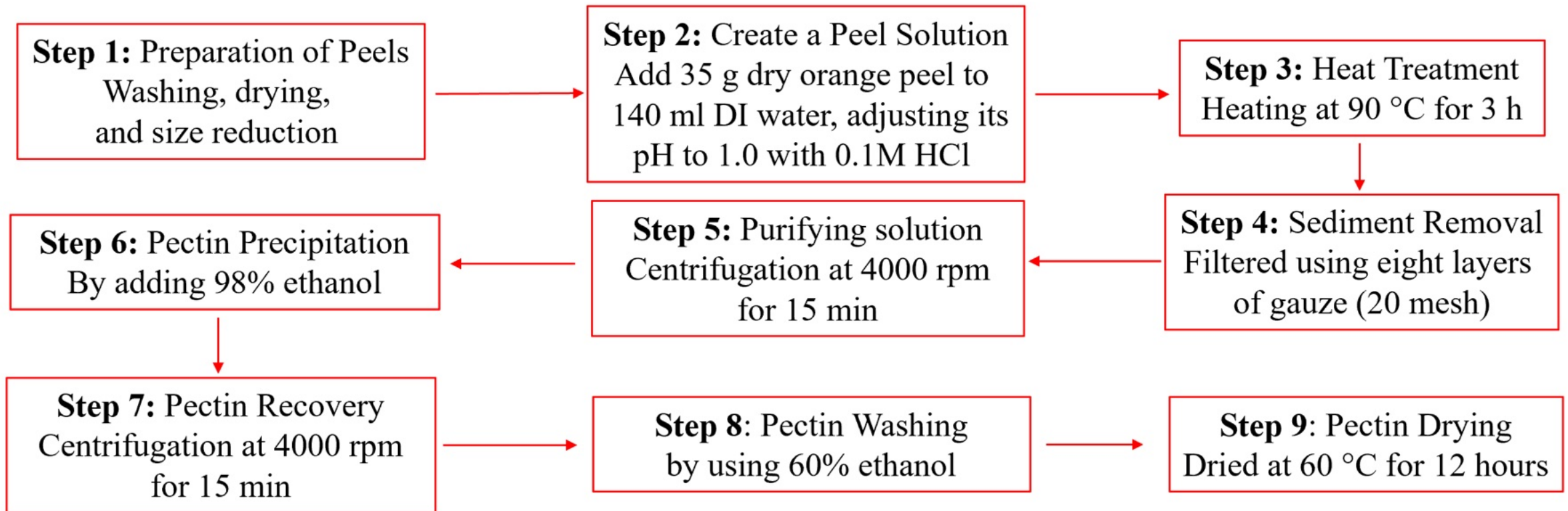
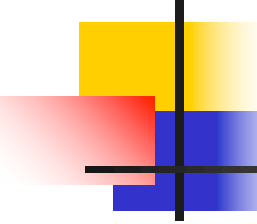


Illustration of Pectin extraction from Citrus Peels

A decorative graphic on the left side of the slide consists of overlapping colored squares (yellow, red, blue) and a black crosshair.

Task 1: Design and Synthesis of Green Inhibitors

Pectin extraction procedures

- Cut , wash and dry the orange peels
- Weigh 45 grams of the orange peel
- Add 500 ml of water to the cut peels and add HCl acid to make the solution Ph1
- Heating in a beaker for 3 Hours with continuous stirring for 90°C
- The HCl helps break cell walls of the orange where the pectin is
- Filtration of the solution
- Centrifugation at 400 rpm for 15mins
- Addition of 60 percent ethanol for purification
- Drying in oven for 4 hrs. at 60 degrees Celsius.

Task 1: Design and Synthesis of Green Inhibitors

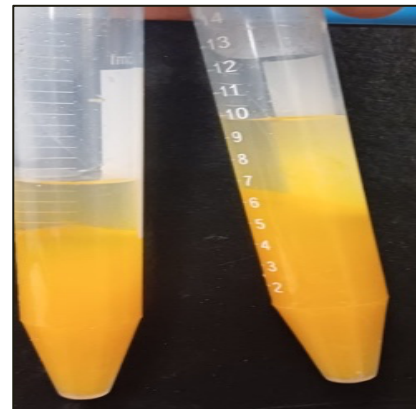
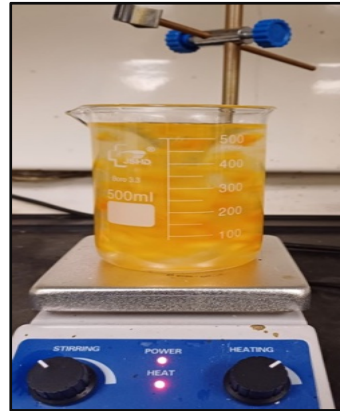
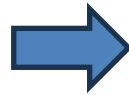
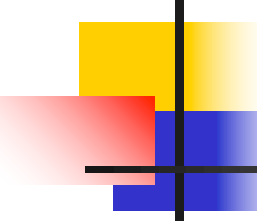


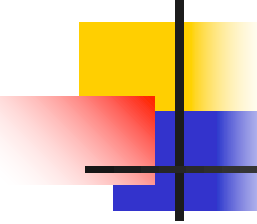
Illustration of pectin extraction procedures

A decorative graphic consisting of overlapping yellow, red, and blue squares with a black crosshair.

Task 1: Design and Synthesis of Green Inhibitors

Surface modification of pectin using amine groups

- Pectin molecules contain carboxyl groups (-COOH) along their backbone.
- EDC and NHS are used to activate these carboxyl groups, making them more reactive and capable of forming stable amide bonds with primary amines present in other molecules
- By activating these functional groups, pectin molecules become more reactive and capable of forming strong covalent bonds with other molecules or surfaces.
- This enhanced reactivity allows pectin to better adhere to various substrates, including metals, polymers, and biological materials



Task 1: Design and Synthesis of Green Inhibitors

- The formation of covalent bonds through the activation of carboxyl and amine groups provides a more stable and durable adhesion compared to physical or weak chemical interactions alone.
- This can lead to improved adhesion strength, resistance to mechanical stress, and long-term stability of pectin-based coatings or modifications.
- 1-Ethyl-3-(3-dimethylaminopropyl) carbodiimide is a water-soluble carbodiimide.
- It is typically employed in the 4.0-6.0 pH range. It is generally used as a carboxyl activating agent for the coupling of primary amines to yield amide bonds.
- N-hydroxy succinimide (NHS), selectively activates the carboxyl groups of pectin without significantly modifying other functional groups present in the molecule.
- pectin molecules contain carboxyl (-COOH) functional groups along their backbone. These carboxyl groups are relatively unreactive under normal conditions. NHS reacts with the carboxyl group of pectin, forming an NHS ester intermediate.
- The NHS ester intermediate is highly reactive toward primary amines

Task 1: Design and Synthesis of Green Inhibitors

Chitosan

- Chitosan is a polysaccharide derived from chitin, which is found in the exoskeletons of crustaceans like shrimp, crab, and lobster.
- It consists of repeating units of glucosamine and N-acetylglucosamine linked by β -(1 \rightarrow 4) glycosidic bonds.
- Chitosan is composed of long chains of these units, which can vary in molecular weight depending on the source and method of extraction.
- It's known for its biocompatibility, biodegradability, and various applications in industries such as pharmaceuticals, food, and cosmetics.

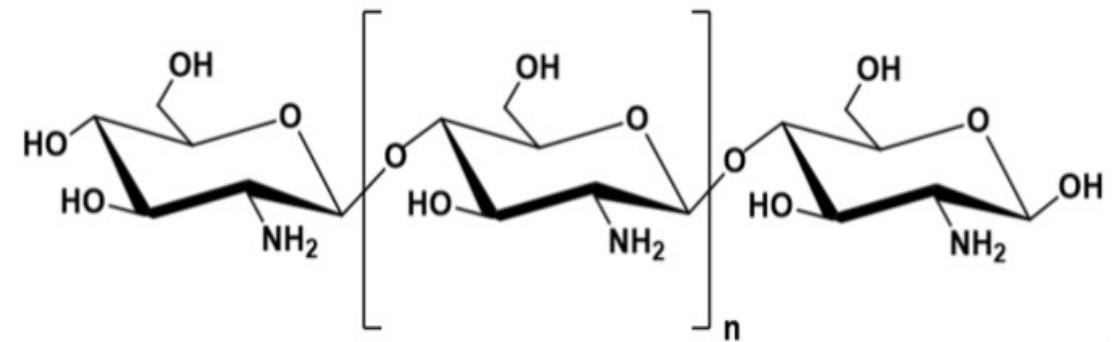
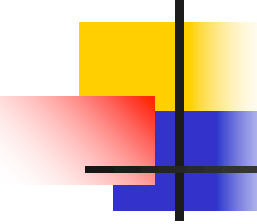


Illustration of the molecular formula of Chitosan.

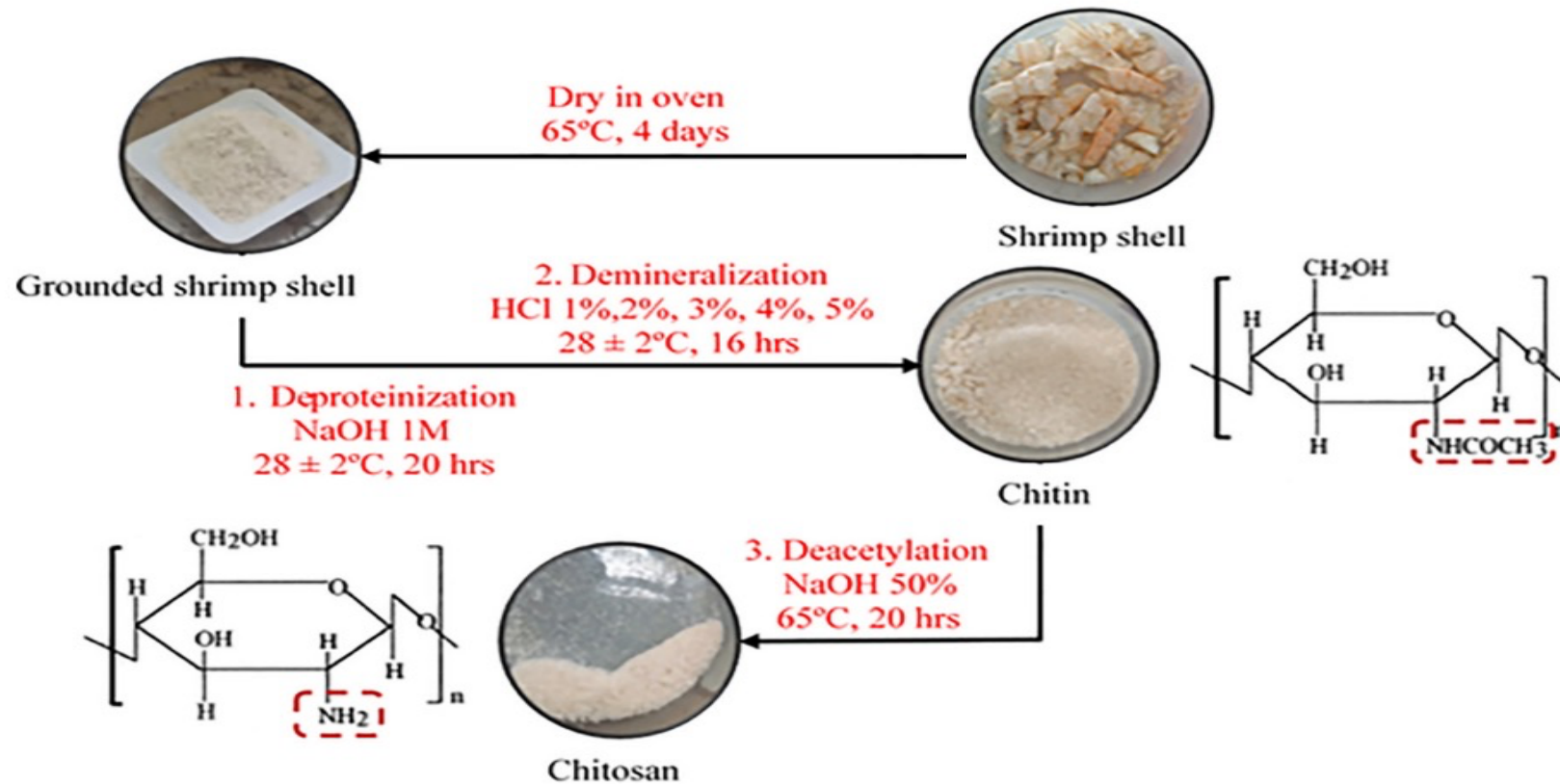
A decorative graphic consisting of overlapping yellow, red, and blue squares with a black crosshair.

Task 1: Design and Synthesis of Green Inhibitors

Chitosan extraction procedures

- **Deproteinization:** This process involves the removal of proteinaceous material from the exoskeleton, leaving behind the chitin matrix. The presence of proteins in shrimp shells can interfere with the isolation and purification of chitin. These proteins can form complexes with chitin, making it difficult to separate and purify the chitin. Sodium hydroxide is used for deproteinization.
- **Demineralization:** Shrimp shells contain not only chitin but also minerals such as calcium carbonate. Demineralization involves removing these mineral components, typically through the use of acidic solutions like hydrochloric acid or acetic acid.
- **Deacetylation:** Removal of alkyl group COCH_3 to convert from chitin to chitosan using strong NaOH solution.

Task 1: Design and Synthesis of Green Inhibitors



Hisham, F., Akmal, M. M., Ahmad, F. B., & Ahmad, K. (2021). Facile extraction of chitin and chitosan from shrimp shell. *Materials Today: Proceedings*, 42, 2369-2373.

Task 1: Design and Synthesis of Green Inhibitors

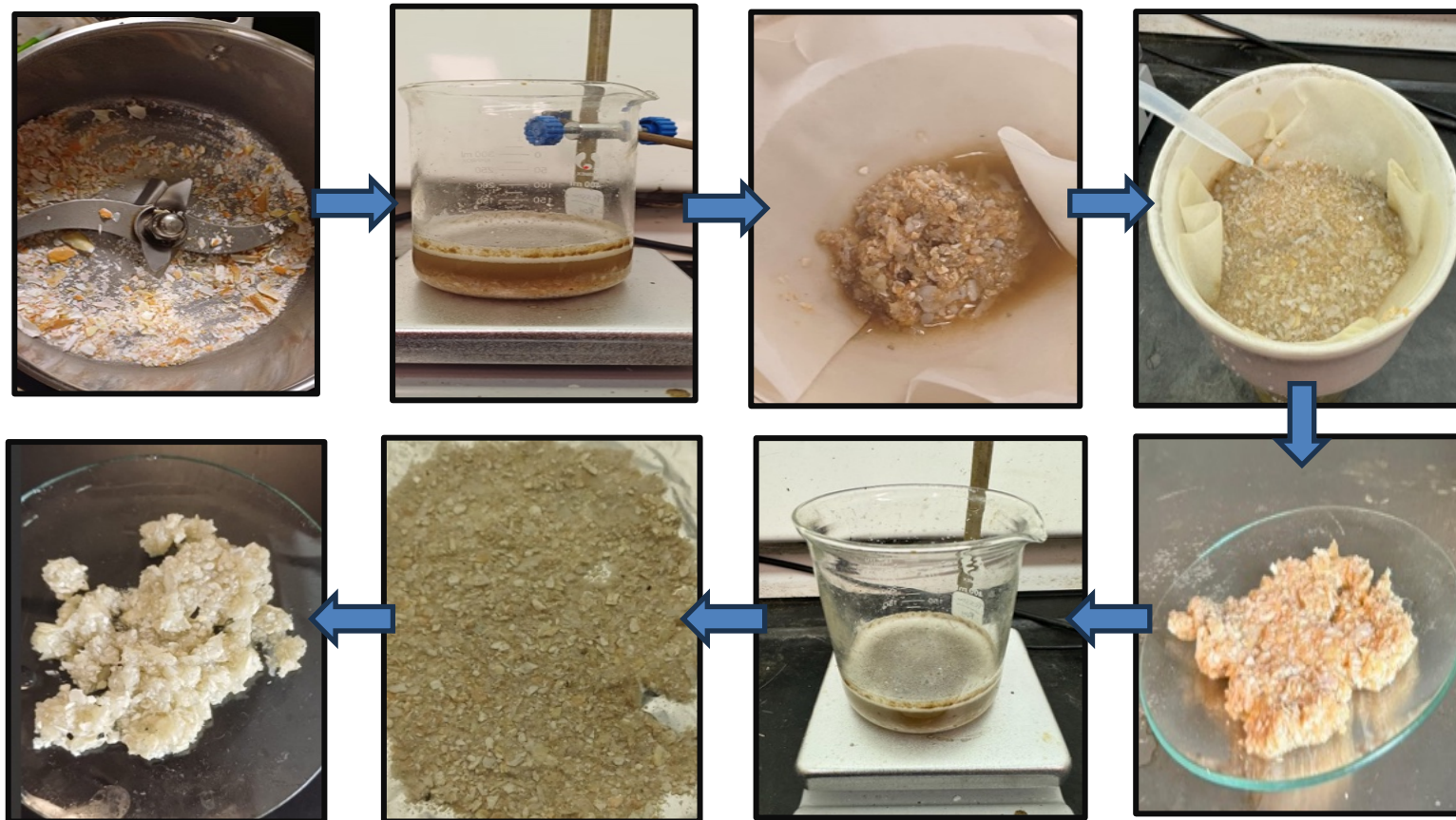
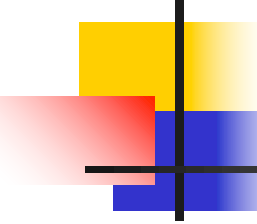


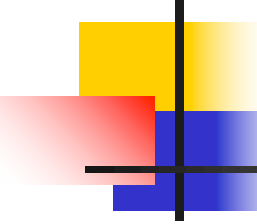
Illustration of Chitosan extraction procedures

A decorative graphic consisting of overlapping yellow, red, and blue squares with a black crosshair.

Task 1: Design and Synthesis of Green Inhibitors

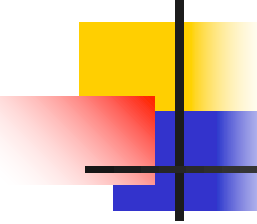
Extraction of Chitosan from shrimp shells

- Ground shrimp shells, washed and dried in an oven at 65 °C
- Deproteinization of the shrimp cells with NaOH solution
- 15 g of shrimp cell powder mixed in 75 ml of NaOH solution (1:5 w/v ratio)
- Heating and stirring this mixture at 30°C for 20 hours
- Filtering the solution
- Washing with water until the pH turns to 7 (neutral).
- Drying in oven overnight at 60 °C.

A decorative graphic on the left side of the slide, consisting of overlapping yellow, red, and blue squares with a black crosshair.

Task 1: Design and Synthesis of Green Inhibitors

- Demineralization of the shrimp cells using HCl acid
- Dried shrimp cells obtained from Deproteinization mixed in Hcl acid solution
- Shrimp cells immersed in 2 percent HCl solution for 16 hrs at 30°C with continuous stirring
- Filtered and washed with water to obtain a neutral pH.
- Dried overnight in oven to obtain chitin
- Deacetylation for removal of an acetyl group from chitin using a strong NaOH solution
- Chitin mixed in strong 50 percent NaOH solution for 20hrs at 60 °C
- Washed to get neutral Ph and dried in an oven for 15 hours to get Chitosan.

A decorative graphic on the left side of the slide, consisting of overlapping yellow, red, and blue squares with a black crosshair.

Task 1: Design and Synthesis of Green Inhibitors

Modification of Chitosan (literature)

- By a simple and convenient method of using formaldehyde as linkages, two new chitosan (CS) derivatives modified respectively with thiosemicarbazide (TSFCS) and thiocarbohydrazide (TCFCS) were synthesized
- Thiosemicarbazide (TS) and thiocarbohydrazide (TC) are organic compounds commonly used in the modification of chitosan for various applications, including metal surface coating and functionalization.
- TS is a compound containing both a thioamide group ($-C=S-NH_2$) and an amino group ($-NH_2$). Its chemical structure allows it to form covalent bonds with chitosan and metal surfaces.
- In chitosan modification, TS acts as a crosslinking agent, linking chitosan molecules together or binding chitosan to other molecules or surfaces.
- TC is another compound used in chitosan modification for metal surface adhesion. It contains a hydrazide group ($-NH-NH_2$) and a thiol group ($-SH$), enabling it to interact with chitosan and metal surfaces.
- Similar to TS, TC acts as a crosslinking agent and adhesive promoter for chitosan.

Results

- The preliminary results show that the new compound TCFCS can act as a mixed-type metal anticorrosion inhibitor, its inhibition efficiency is 92% when the concentration is 60 mg/L.

Li, M., Xu, J., Li, R., Wang, D., Li, T., Yuan, M., & Wang, J. (2014). Simple preparation of aminothiourea-modified chitosan as corrosion inhibitor and heavy metal ion adsorbent. Journal of colloid and interface science, 417, 131-136.

Task 1: Design and Synthesis of Green Inhibitors

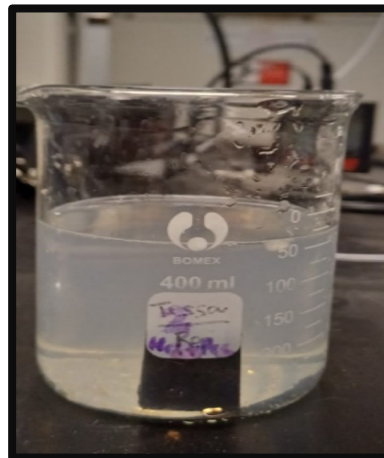
Weight loss corrosion test

- Preparation of 1M HCl sample using 37 percent AR grade HCl solution.
- Preparation of 3 samples
- Sample 1: Pure HCl 1M solution
- Sample 2: Pectin solution (0.2 gm in 100 ml water) mixed with pure HCl
- Sample 3: Dip-coated metal in pectin solution (0.4 gm in 100 ml water) dipped in HCl.

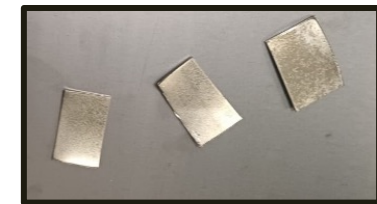
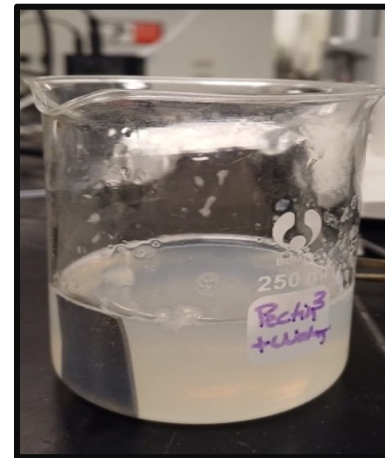
Sample 1



Sample 2



Sample 3



Cut carbon steel samples

Task 1: Design and Synthesis of Green Inhibitors

Initial results on pectin

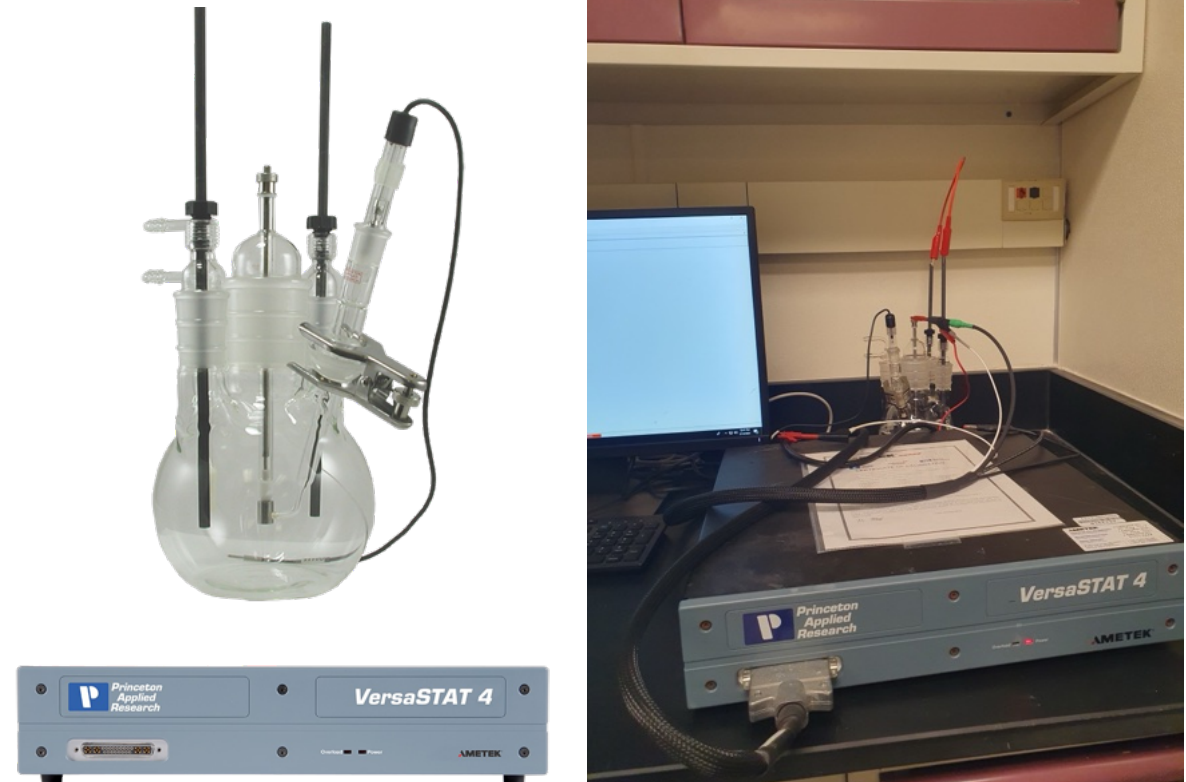
Corrosion medium: 1M HCl solution, Duration: 24 hours, T: 25 °C, Beakers in fume hood to minimize oxygen contact. Pectin dissolved in water (2 gL⁻¹), Area of exposure 7.5 cm²

Parameters	Sample 1	Sample 2	Sample 3
Steel sample	Carbon steel	Carbon steel	Carbon steel
Weight before corrosion (g)	7.451	7.837	6.288
Weight after corrosion (g)	7.363	7.804	6.238
Pectin application	No	Pectin solution in HCl	Dip coating
Weight loss (g)	0.088	0.033	0.055
Corrosion percentage(%)	1.18%	0.423%	0.79%
Inhibitor efficiency	-	62.5% at 25°C	33% at 25 °C

Task 1: Design and Synthesis of Green Inhibitors

Electrochemistry corrosion test

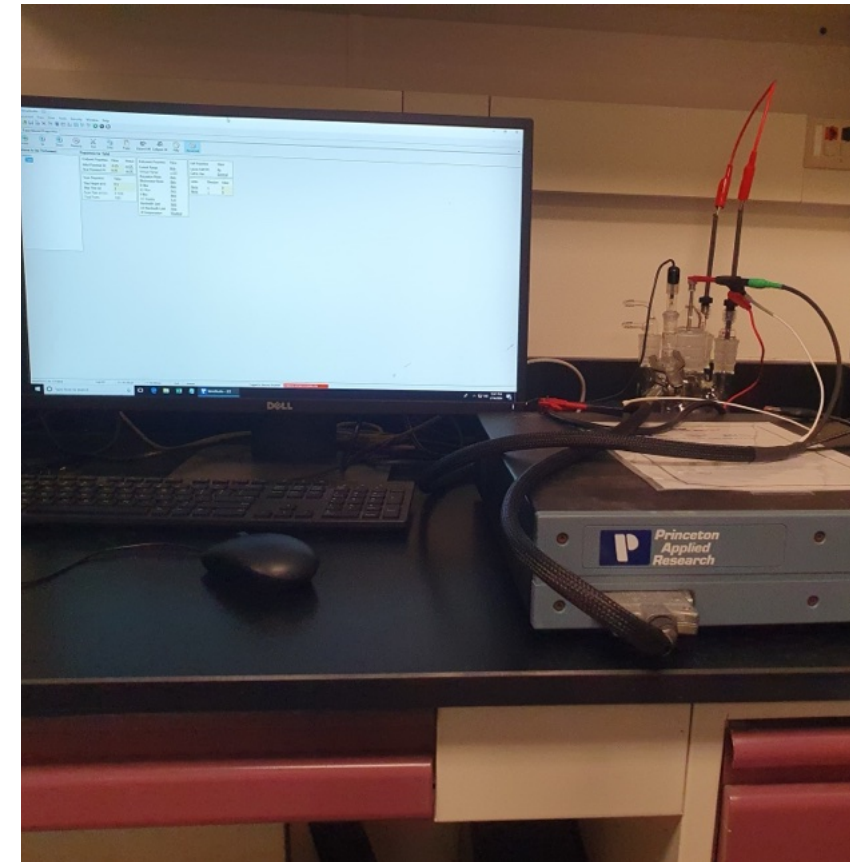
A three-electrode cell will be used for the electrochemical studies via a potentiostat (VersaSTAT 4, ameteksi Instruments). In this setup, the carbon steel will act as the working electrode, while the reference electrode is the Saturated Calomel Electrode (SCE). A graphite electrode will be used as a counter electrode.



Task 1: Design and Synthesis of Green Inhibitors

Electrochemistry corrosion test

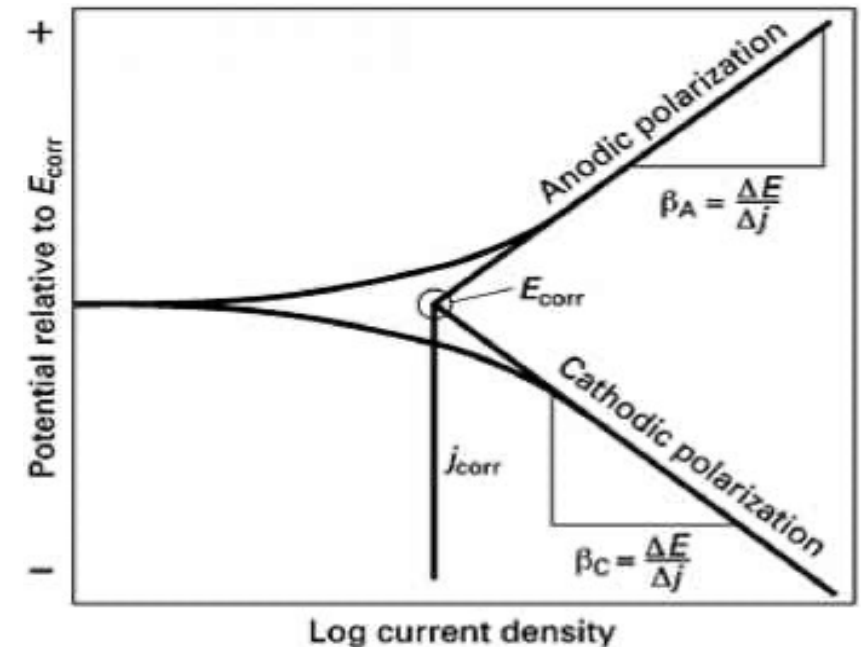
- Two electrochemical corrosion tests:
 - Polarization techniques
 - Electrochemical impedance spectroscopy (EIS)
- Different corrosive media
 - HCl
 - SO₂
 - CO₂ (Sweet corrosion)
 - H₂S (Sour corrosion)
 - H₂SO₄
- Different inhibitor concentrations and coated samples.



Task 1: Design and Synthesis of Green Inhibitors

Polarization techniques

- Polarization techniques encompass several methods, including Tafel extrapolation, potentiodynamic measurements, cyclic polarization, and linear polarization resistance.
- Tafel extrapolation involves a **destructive** test. By examining extrapolation plots, any changes in the corrosion mechanism can be discerned through variations in the Tafel slope. Additionally, a direct measurement of the corrosion current is obtained.
- When a metallic electrode is immersed in a corrosive medium, anodic and cathodic reactions spontaneously occur on the electrode surface, triggering corrosion.



Task 1: Design and Synthesis of Green Inhibitors

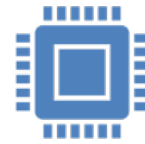
Electrochemical impedance spectroscopy



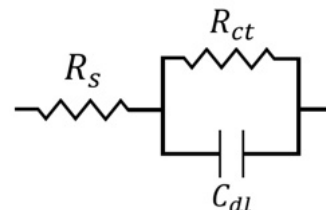
Electrochemical Impedance Spectroscopy (EIS) is a non-destructive experimental technique that captures the response of a nonlinear electrochemical system as a function of applied potential. It provides valuable information about the metal/electrolyte interface.



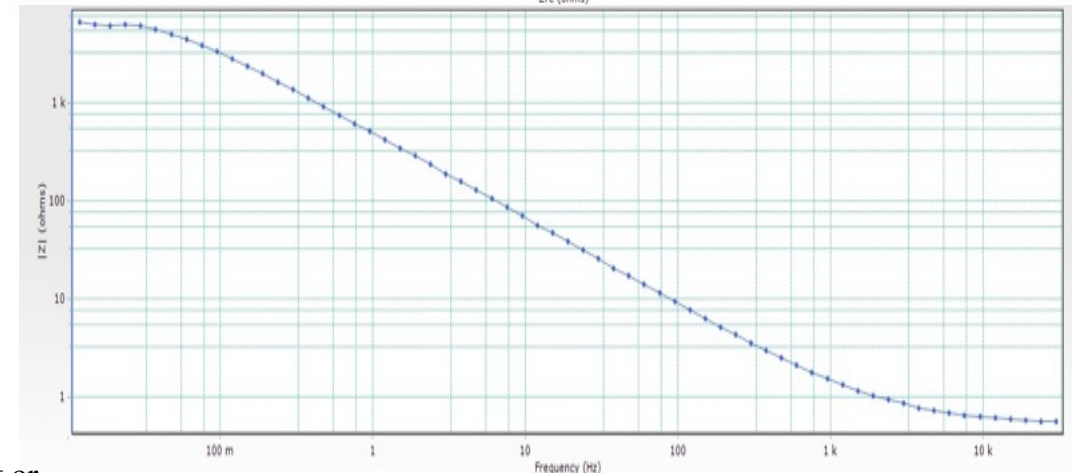
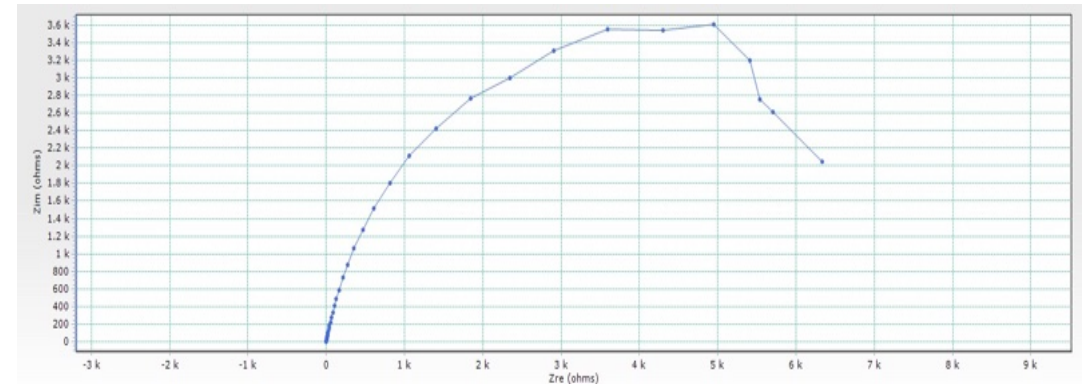
Within short testing times, EIS measurements yield reliable data, enabling us to predict the long-term performance of inhibitors. The result of EIS is the impedance of the electrochemical system as a function of frequency.



We have the option to analyze EIS data using the common electrical equivalent circuit (EEC) approach, as well as with physics-based/mechanistic models.



Electrical equivalent circuit or Randles Circuit



Task 1: Design and Synthesis of Green Inhibitors

Electrochemical impedance spectroscopy



Experimental Procedure for EIS Technique:



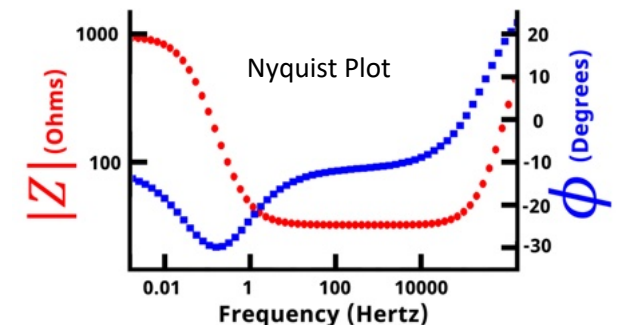
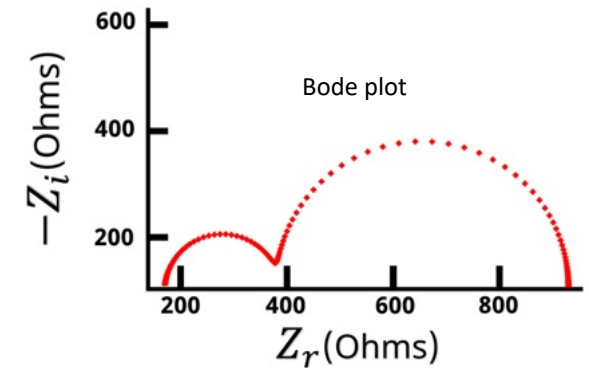
Measurements are carried out over a broad frequency range from 100 kHz to 0.01 Hz using sinusoidal AC perturbation with amplitude of 5 mV.

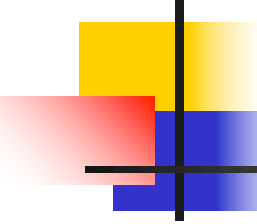


Once the potentiostat collects the potential vs. time and the current vs. time data at each frequency, a Fast Fourier Transform (FFT) is applied to the data. The FFT converts the potential vs. time and current vs. time into potential magnitude vs. frequency and current magnitude vs. frequency.



The potential amplitude E_0 , current amplitude i_0 , and the phase angle Φ_i at each frequency f are determined from the FFT analysis. With these data we can describe the different plotting conventions associated with EIS.

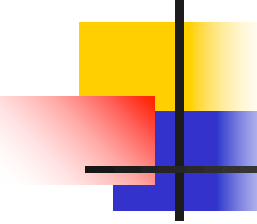


A decorative graphic on the left side of the slide consists of overlapping colored squares (yellow, red, blue) and a black crosshair.

Task 1: Design and Synthesis of Green Inhibitors

Work plan for Q3

- Continue functionalizing/modifying pectin
- Synthesize and modify chitosan-derived inhibitors
- Establish baseline corrosion data for chemical-based inhibitors
- Evaluate pectin and chitosan inhibitors
- Build a database for all inhibitors (chemicals and green ones)

A decorative graphic consisting of overlapping yellow, red, and blue squares with a black crosshair.

Task 1: Design and Synthesis of Green Inhibitors

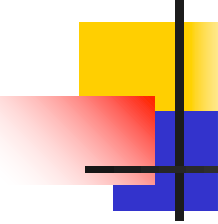
Reference

Fazal, Basit Raza, et al. "A review of plant extracts as green corrosion inhibitors for CO₂ corrosion of carbon steel." *npj Materials Degradation* 6.1 (2022): 5.

Shang, Zheng, and Jinyang Zhu. "Overview on plant extracts as green corrosion inhibitors in the oil and gas fields." *Journal of Materials Research and Technology* 15 (2021): 5078-5094.

Hisham, F., Akmal, M. M., Ahmad, F. B., & Ahmad, K. (2021). Facile extraction of chitin and chitosan from shrimp shell. *Materials Today: Proceedings*, 42, 2369-2373.

Li, M., Xu, J., Li, R., Wang, D., Li, T., Yuan, M., & Wang, J. (2014). Simple preparation of aminothiourea-modified chitosan as corrosion inhibitor and heavy metal ion adsorbent. Journal of colloid and interface science, 417, 131-136.

A decorative graphic on the left side of the slide consisting of overlapping yellow, red, and blue squares with a black crosshair.

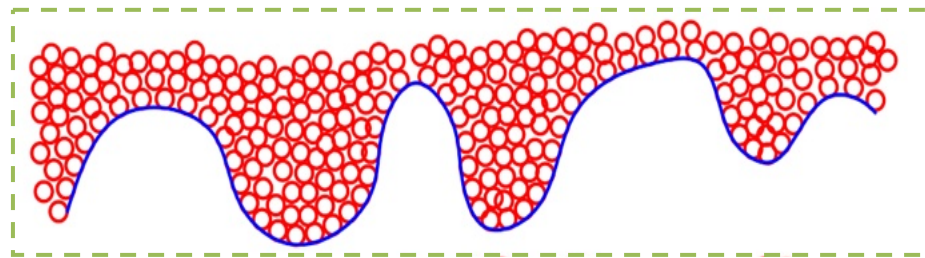
Task 2: Simulation-based Inhibitor Implementation Optimization in Gas Gathering and Transportation Pipelines

Progress made in Q2

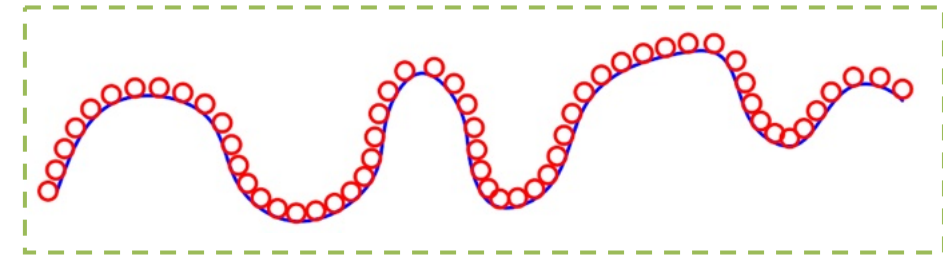
- Develop the inhibitor degradation mechanism model with wall shear stress (WSS)
- Develop Fourier operator network to predict WSS
- Develop a multi-fidelity model using a convolutional neural network for computational efficiency

Task 2: Simulation-based Inhibitor Implementation Optimization in Gas Gathering and Transportation Pipelines

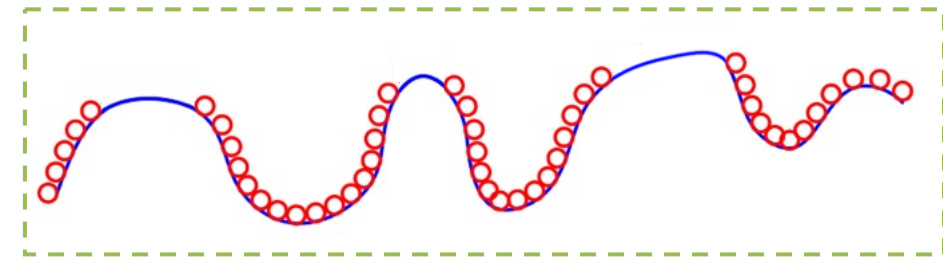
Task 2.1: Physics-guided inhibitor degradation prediction model



Initially added inhibitor on the pipe wall



Stably distributed Inhibitor film



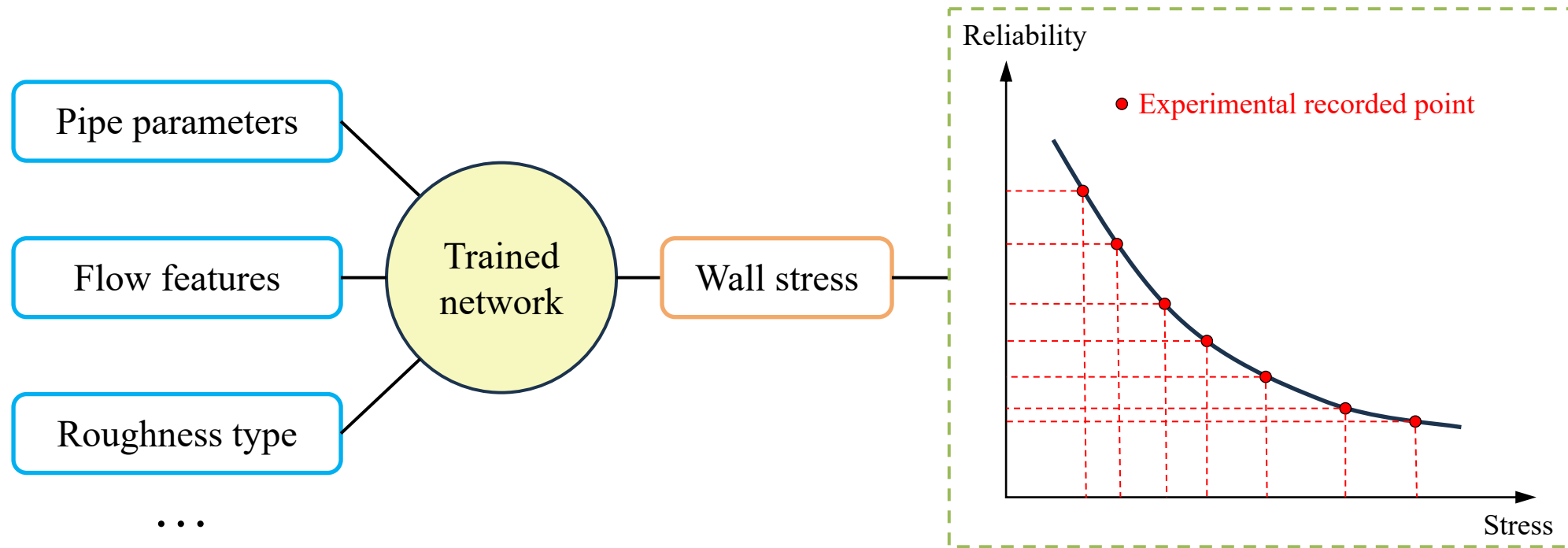
Inhibitor degradation and adhesion loss

Research objects

- Surrogate model for predicting near-wall stress.
- Effects of wall shear stress on inhibitor degradation;

Task 2: Simulation-based Inhibitor Implementation Optimization in Gas Gathering and Transportation Pipelines

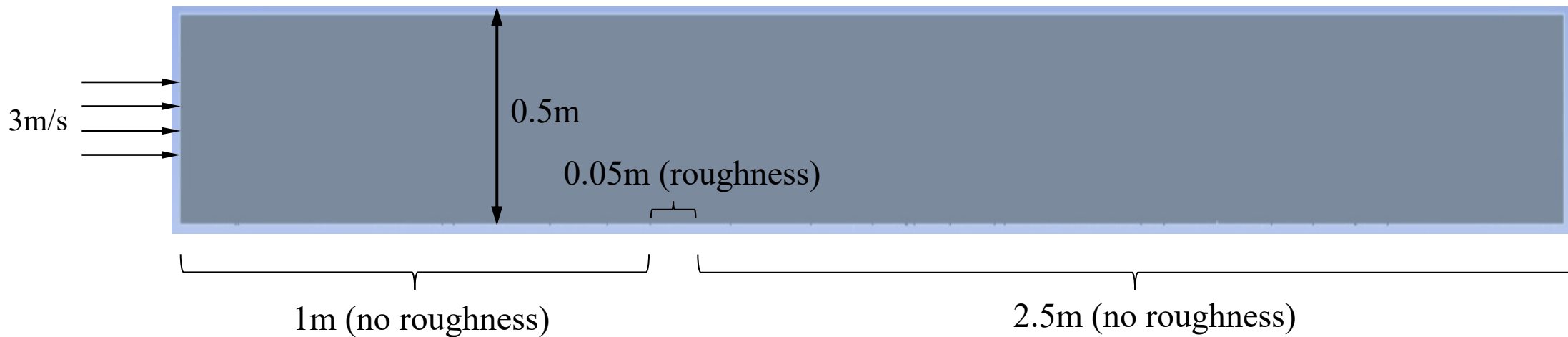
Task 2.1: Physics-guided inhibitor degradation prediction model



Schematic illustration of predicting inhibitor degradation.

Task 2: Simulation-based Inhibitor Implementation Optimization in Gas Gathering and Transportation Pipelines

Task 2.1: Physics-guided inhibitor degradation prediction model



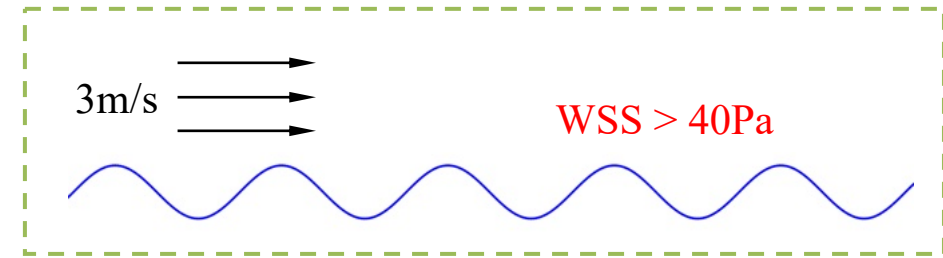
Schematic diagram of the numerical pipe model

Task 2: Simulation-based Inhibitor Implementation Optimization in Gas Gathering and Transportation Pipelines

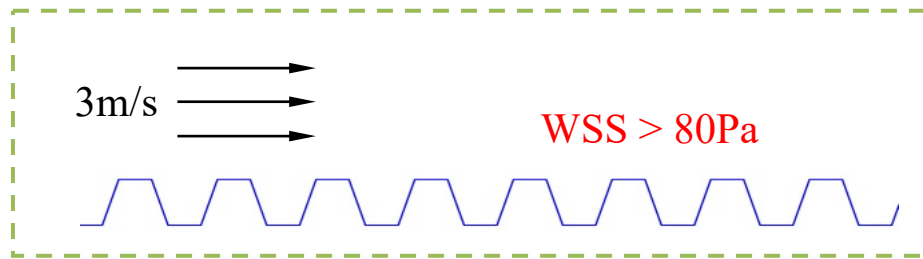
Task 2.1: Physics-guided inhibitor degradation prediction model



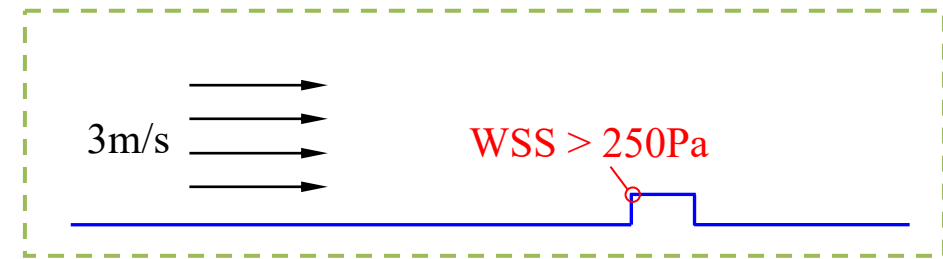
No roughness considered



Sinusoidal roughness



Trapezoidal roughness



1mm protrusion (compared to surrounding heights)

Schematic illustration of the maximum wall shear stress (WSS) under typical roughness.

Task 2: Simulation-based Inhibitor Implementation Optimization in Gas Gathering and Transportation Pipelines

Task 2.1: Physics-guided inhibitor degradation prediction model

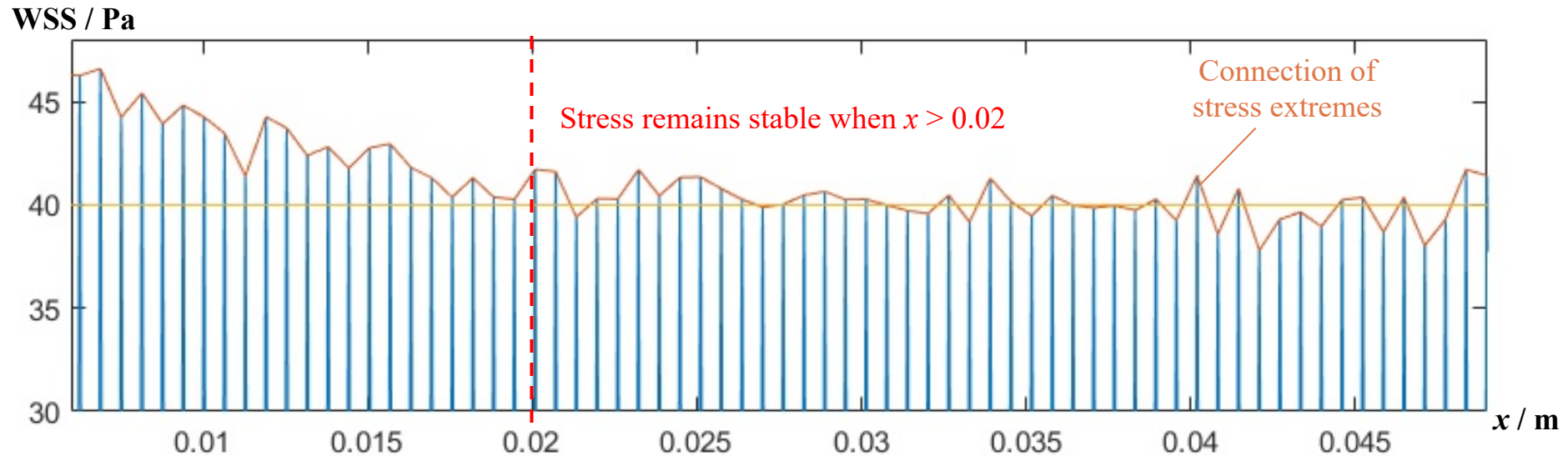


Illustration of selecting data segment with sinusoidal roughness

Task 2: Simulation-based Inhibitor Implementation Optimization in Gas Gathering and Transportation Pipelines

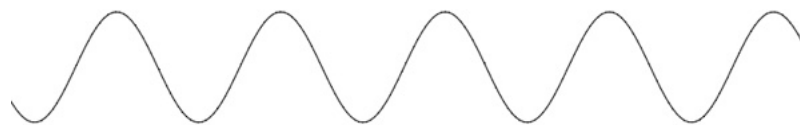
Task 2.1: Physics-guided inhibitor degradation prediction model



$$y=0.14*\cos(0.1*x)+0.14 \text{ (mm)}$$



$$y=0.14*\cos(0.15*x)+0.14 \text{ (mm)}$$



$$y=0.16*\cos(0.1*x)+0.16 \text{ (mm)}$$



$$y= 0.16 *\cos(0.15*x)+0.16 \text{ (mm)}$$

- The **last 8 mm segments** of each roughness model are set as the test data, and the remaining parts are used for training

Illustration of the applied dataset.

Task 2: Simulation-based Inhibitor Implementation Optimization in Gas Gathering and Transportation Pipelines

Task 2.1: Physics-guided inhibitor degradation prediction model

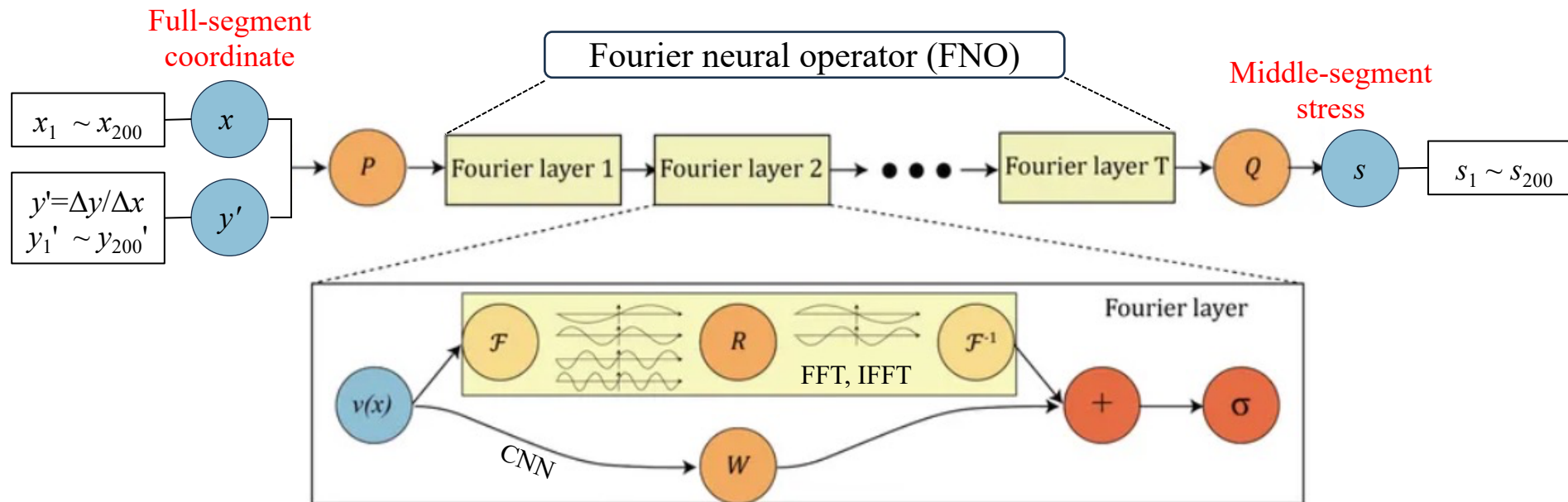


Illustration of FNO network for WSS prediction.

Task 2: Simulation-based Inhibitor Implementation Optimization in Gas Gathering and Transportation Pipelines

Task 2.1: Physics-guided inhibitor degradation prediction model

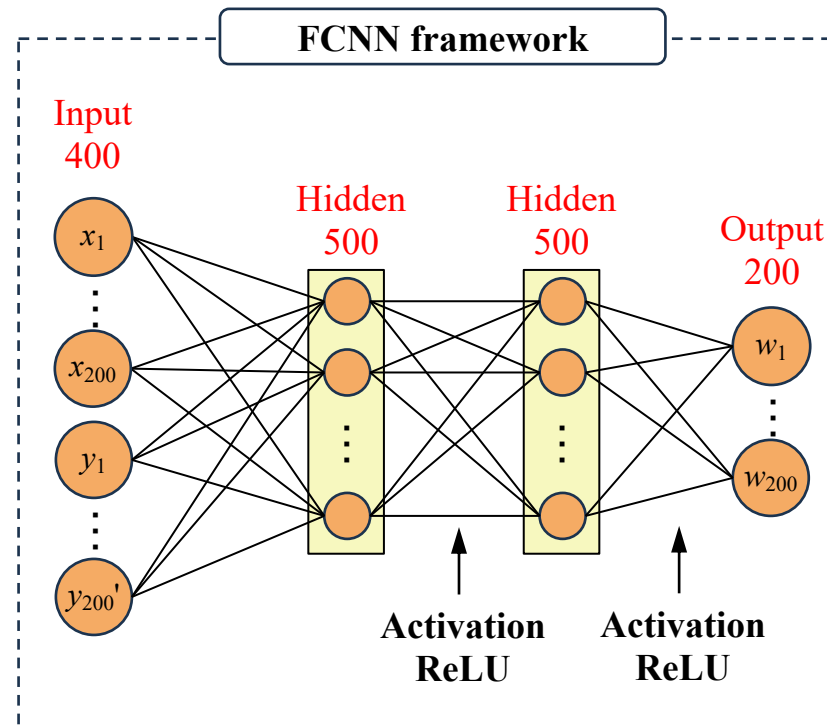


Illustration of the applied fully-connected neural network (FCNN).

Task 2: Simulation-based Inhibitor Implementation Optimization in Gas Gathering and Transportation Pipelines

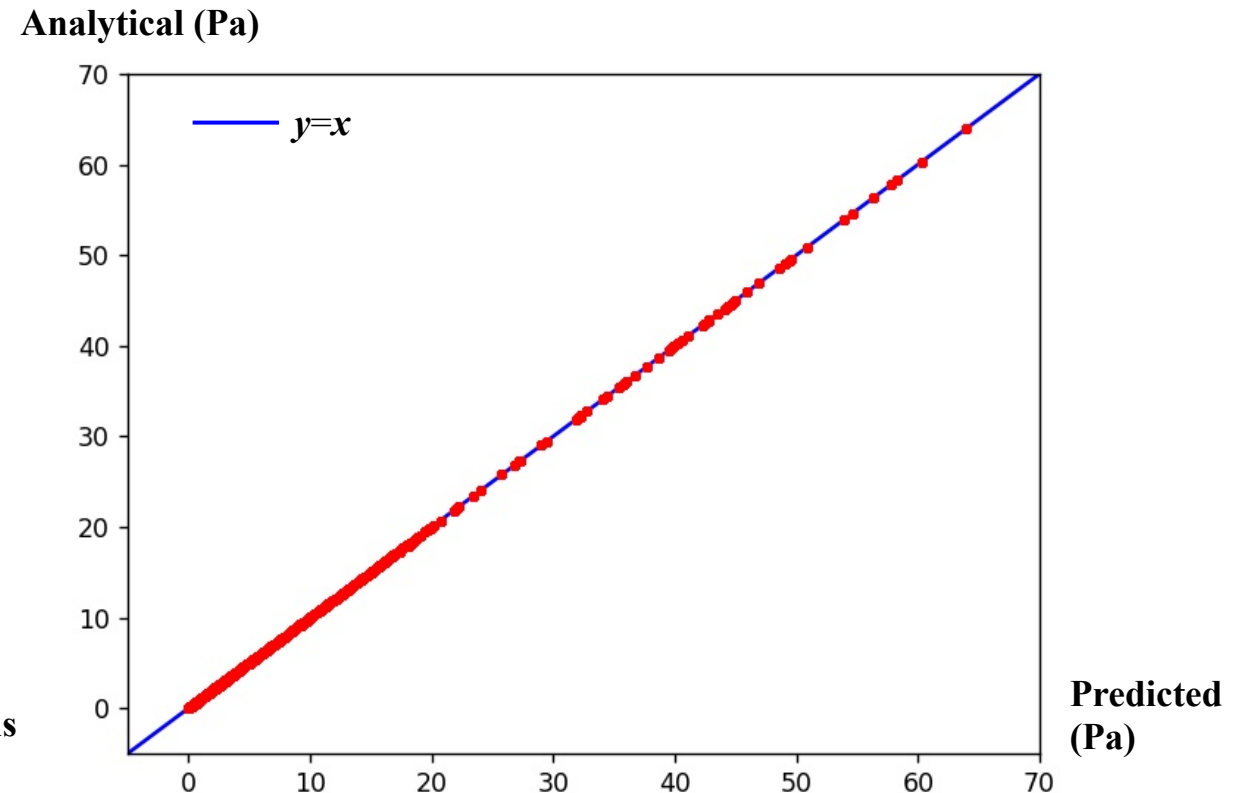
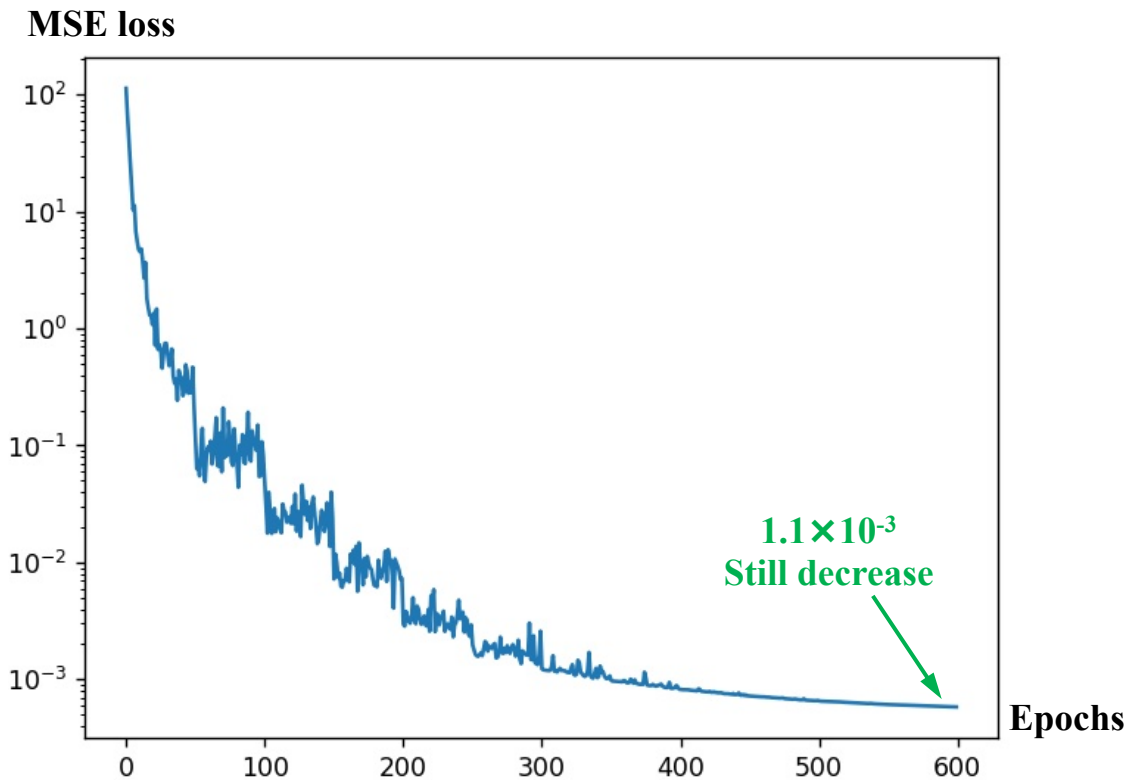
Task 2.1: Physics-guided inhibitor degradation prediction model

	FNO		FCNN
Parameters number	549569	<u>Similar</u>	551200
Epoch number	600		600
Average time consumption in each epoch (s)	2.23	<u>Difference in FFT</u>	0.77
Batch size	1		1
Original learning rate	0.001		0.001
Learning rate decay	0.5 per 50 steps		0.5 per 50 steps

Comparison between the applied FNO and fully-connected network.

Task 2: Simulation-based Inhibitor Implementation Optimization in Gas Gathering and Transportation Pipelines

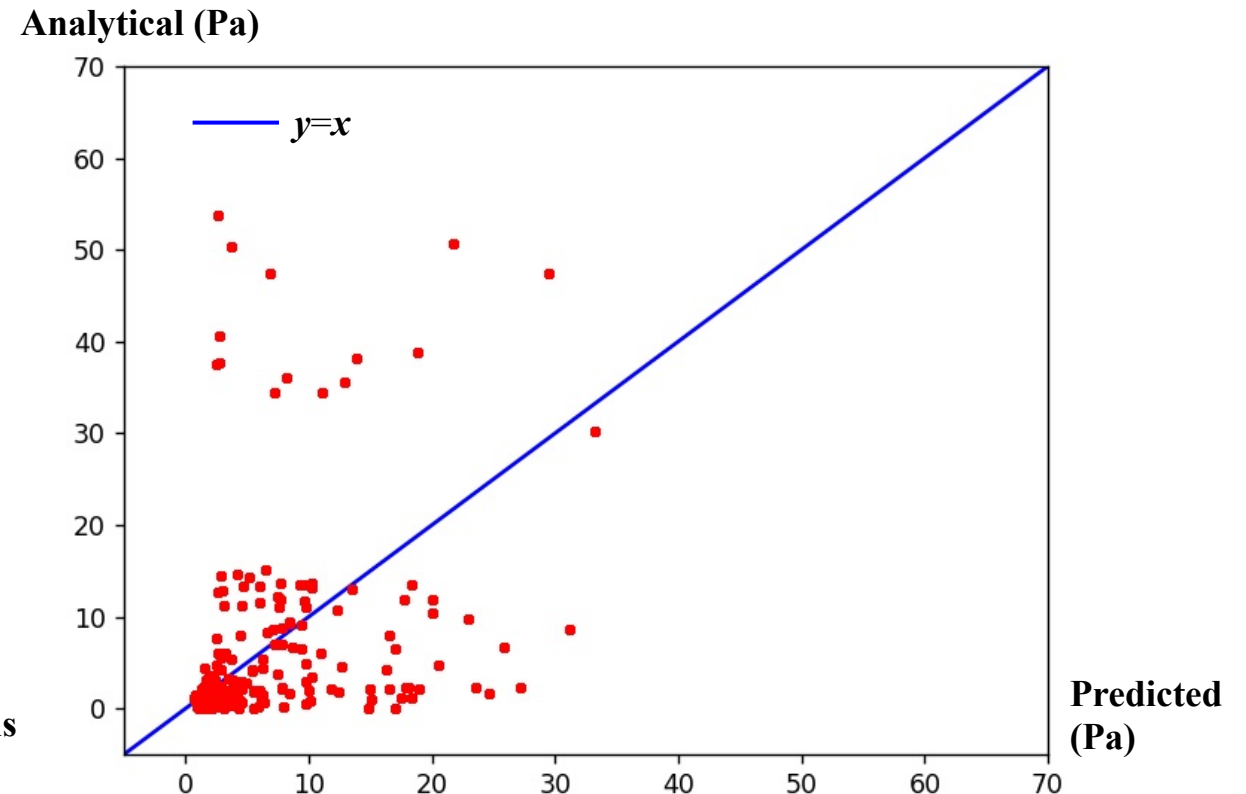
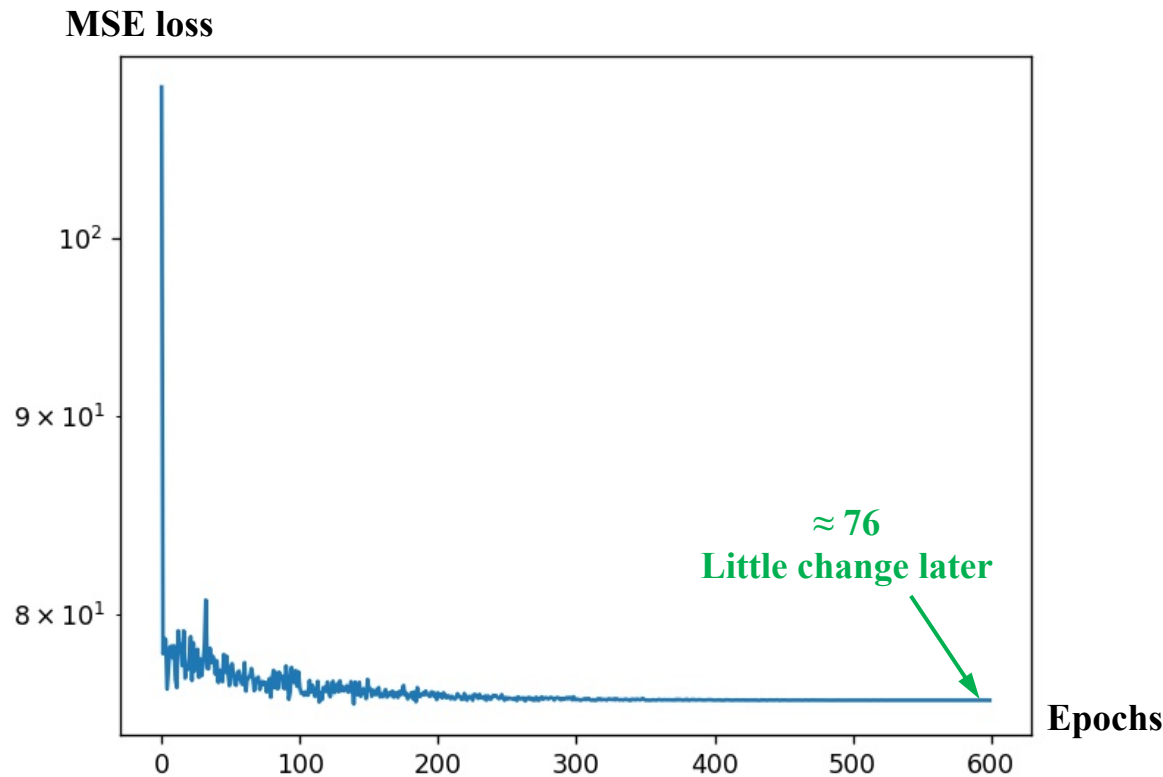
Task 2.1: Physics-guided inhibitor degradation prediction model



Results of predicted WSS with FNO (good prediction).

Task 2: Simulation-based Inhibitor Implementation Optimization in Gas Gathering and Transportation Pipelines

Task 2.1: Physics-guided inhibitor degradation prediction model



Results of predicted WSS with traditional FCNN (bad prediction).

Task 2: Simulation-based Inhibitor Implementation Optimization in Gas Gathering and Transportation Pipelines

Task 2.1: Physics-guided inhibitor degradation prediction model

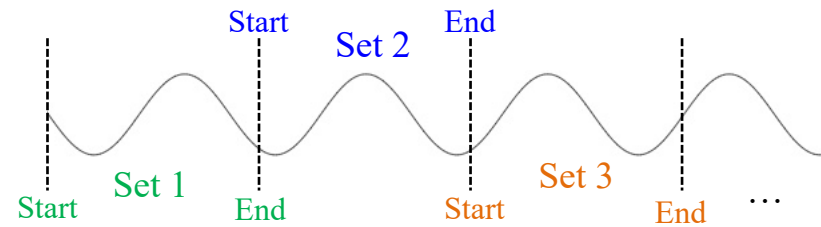


Illustration of data extraction from certain segment.

Difference analysis between FNO and FCNN

- FNO contains the process of Fast Fourier Transform (FFT) and inverse FFT to better identify curve characteristics.
- For random start points and end points from a same segment, FCNN may deem them as different roughness types and fail to learn the similarity among series, while FNO could consider the **arrangement pattern** of data.

Task 2: Simulation-based Inhibitor Implementation Optimization in Gas Gathering and Transportation Pipelines

Task 2.1: Physics-guided inhibitor degradation prediction model

Difficulty in producing dataset: High accuracy requires more high-fidelity modeling for the entire pipe.

- For applied cases, one type of roughness model produces only about 50 sets of training data, requiring 10 mins for meshing, with a mesh size of 3E-5 m in roughness locations;
- To ensure precision, mesh size should be up to 5E-6 m, resulting in more time consumption.

Improvement approaches:

- Using the concept of multi-fidelity modeling to improve the efficiency of simulation
- Use more low-fidelity simulations (less time, less accuracy) and several high-fidelity simulations (more time, more accuracy) to achieve a similar accuracy of high-fidelity

Task 2: Simulation-based Inhibitor Implementation Optimization in Gas Gathering and Transportation Pipelines

Task 2.1: Physics-guided inhibitor degradation prediction model

Governing equation as physical constraint:

- **Navier-Stokes Equation:** $\partial u / \partial t + (u \cdot \nabla) u = -1/\rho \nabla p + \nu \nabla^2 u$
- **Continuity Equation:** $\nabla \cdot u = 0$

u: Velocity (2d vector)

p: Pressure

ν : Kinematic Viscosity

ρ : Density

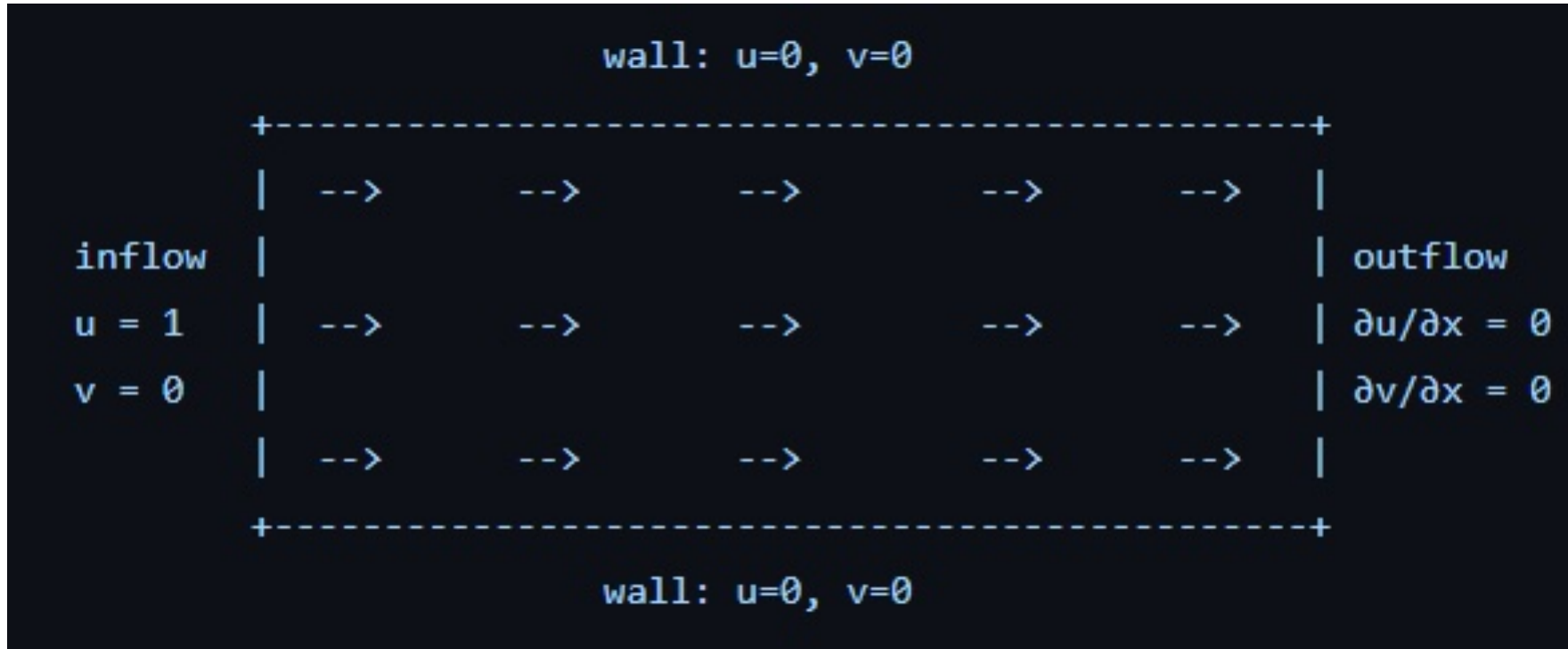
t: Time

∇ : Divergence operator (defining nonlinear convection, gradient and divergence)

∇^2 : Laplace Operator

Task 2: Simulation-based Inhibitor Implementation Optimization in Gas Gathering and Transportation Pipelines

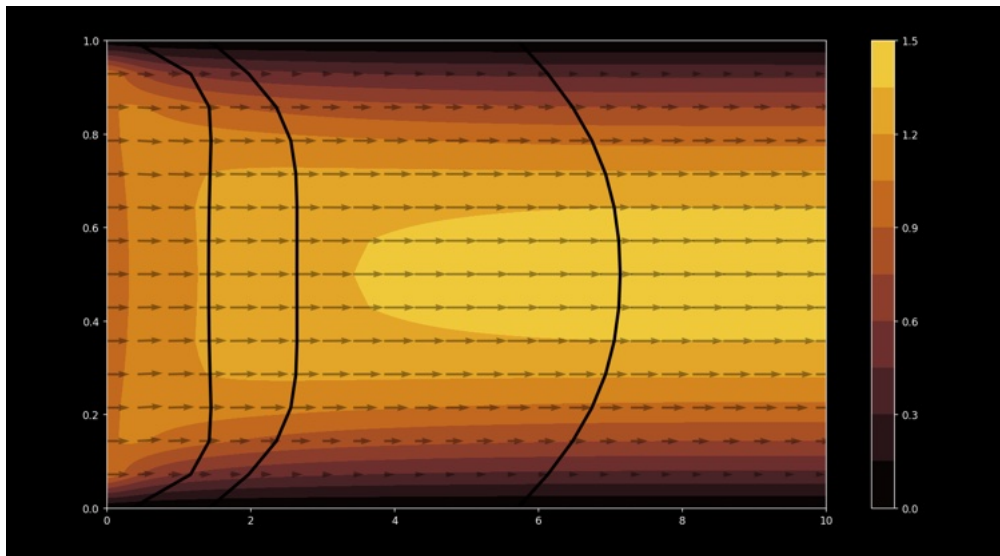
Task 2.1: Physics-guided inhibitor degradation prediction model



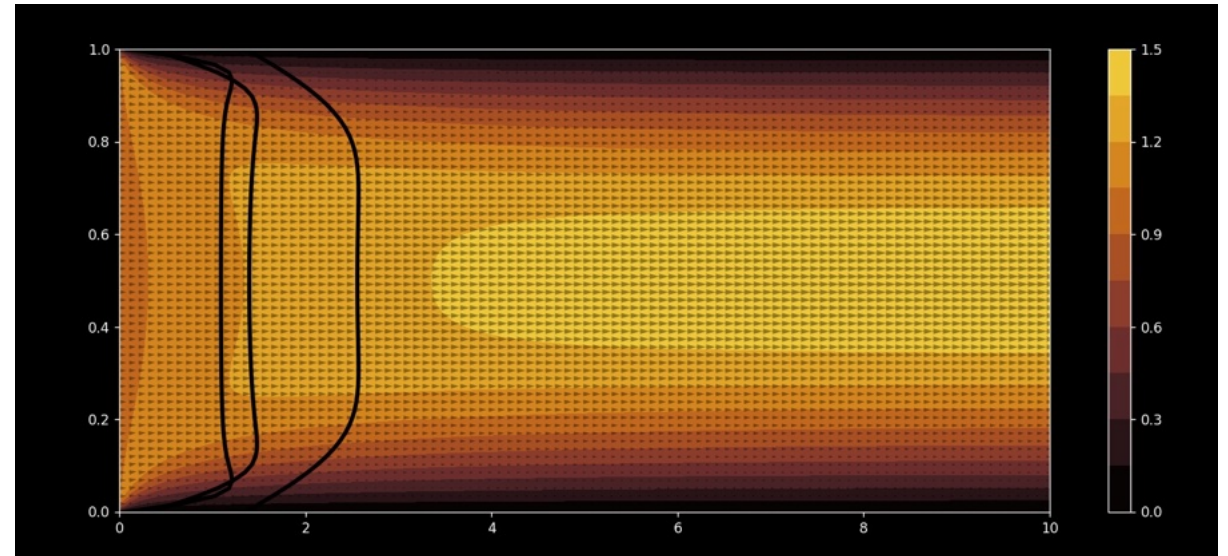
Take a very small “slice” of a pipe where the top and bottom represent wall BCs, the left edge the inlet ($u = 1$ is horizontal velocity) and the right edge the outflow.

Task 2: Simulation-based Inhibitor Implementation Optimization in Gas Gathering and Transportation Pipelines

Task 2.1: Physics-guided inhibitor degradation prediction model

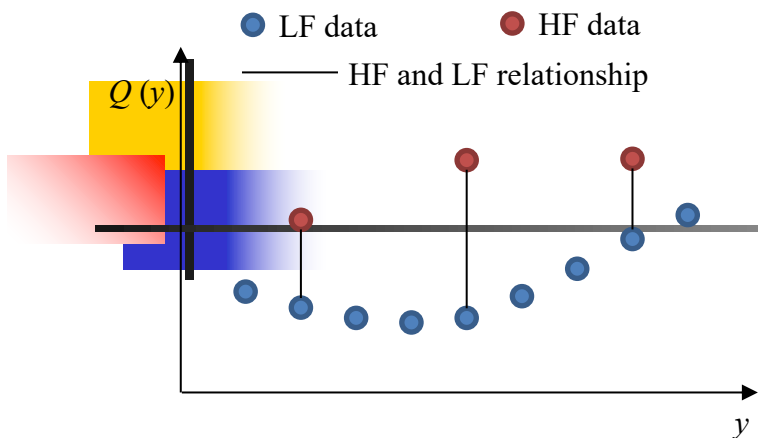


Low fidelity

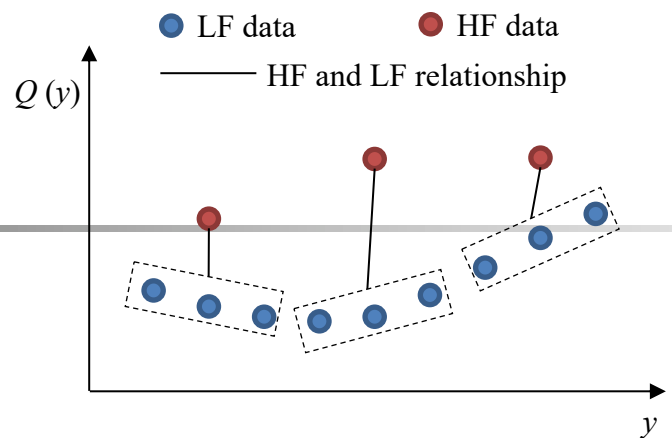


High fidelity

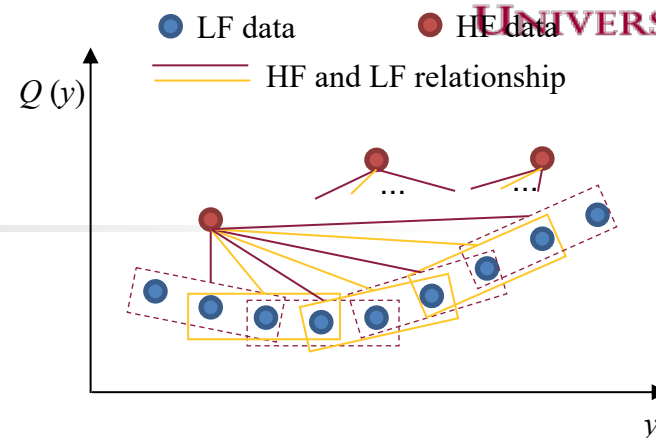
Multi-fidelity Data Aggregation using Convolutional Neural Networks



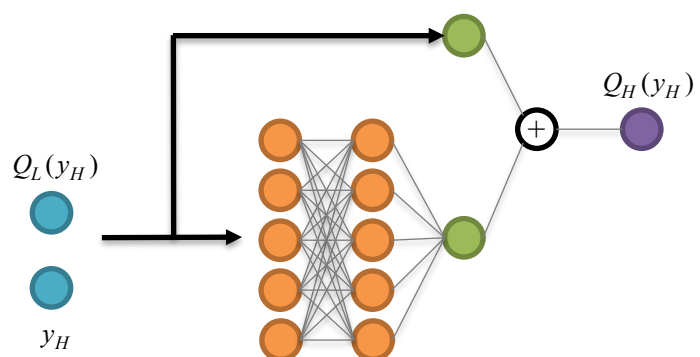
Relationship between HF data and **corresponding LF data**



Relationship between HF data and **neighboring LF data**



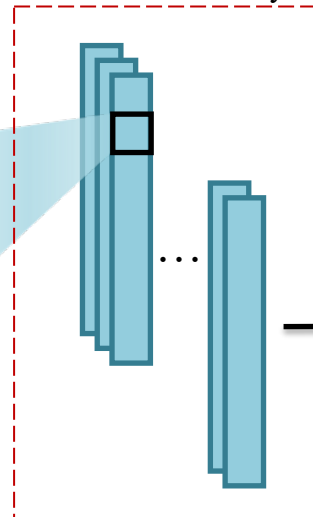
Relationship between HF data and **every LF datum**



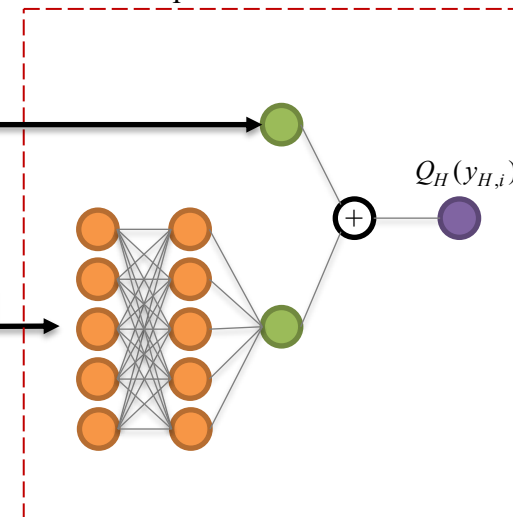
Multi-fidelity data compiling

y_L	$Q_L(y_L)$	$y_{H,i}$	$Q_L(y_{H,i})$
$y_{L,1}$	$Q_L(y_{L,1})$	$y_{H,i}$	$Q_L(y_{H,i})$
$y_{L,2}$	$Q_L(y_{L,2})$	$y_{H,i}$	$Q_L(y_{H,i})$
$y_{L,3}$	$Q_L(y_{L,3})$	$y_{H,i}$	$Q_L(y_{H,i})$
$y_{L,4}$	$Q_L(y_{L,4})$	$y_{H,i}$	$Q_L(y_{H,i})$
...
...
y_{L,N_L}	$Q_{LF}(y_{L,N_L})$	$y_{H,i}$	$Q_L(y_{H,i})$

Convolutional layer



Deep Neural Network



Multi-fidelity Data Aggregation using Convolutional Neural Networks (MDA-CNN)

Task 2: Simulation-based Inhibitor Implementation Optimization in Gas Gathering and Transportation Pipelines

Task 2.1: Physics-guided inhibitor degradation prediction model

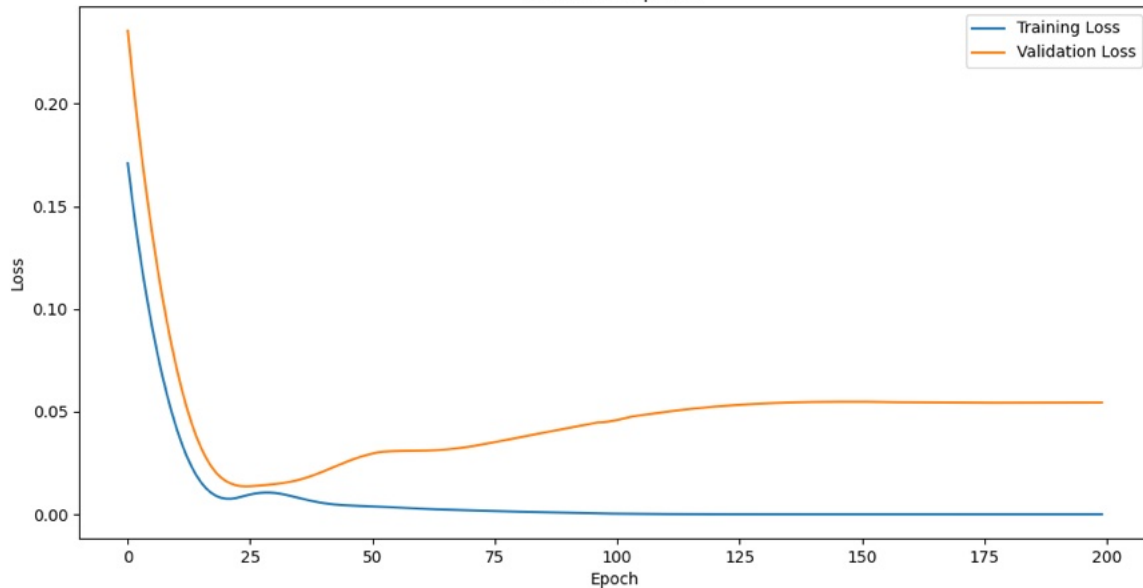
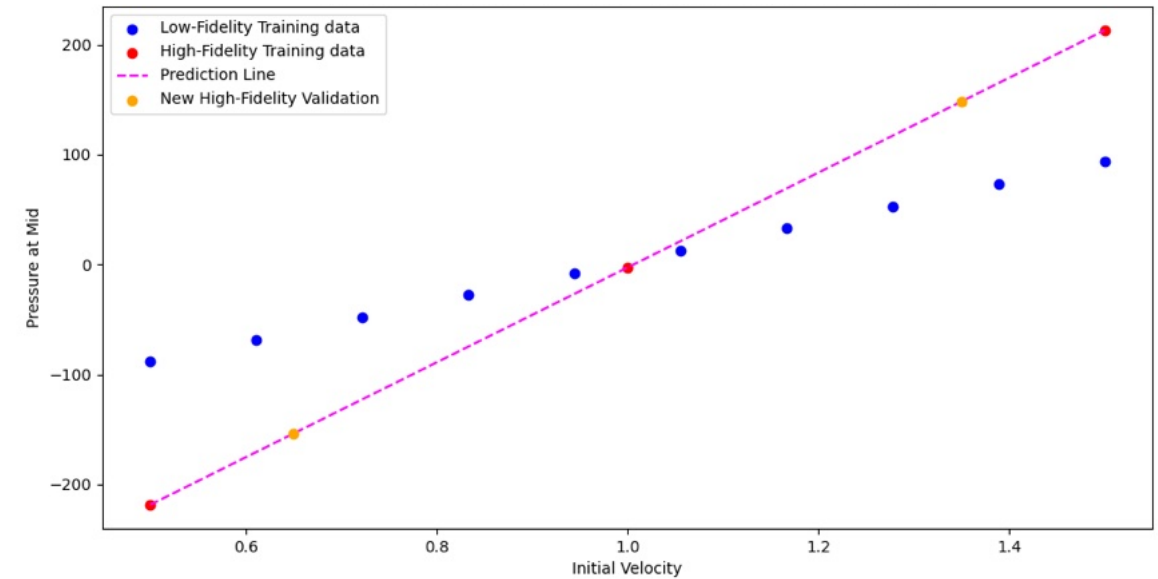


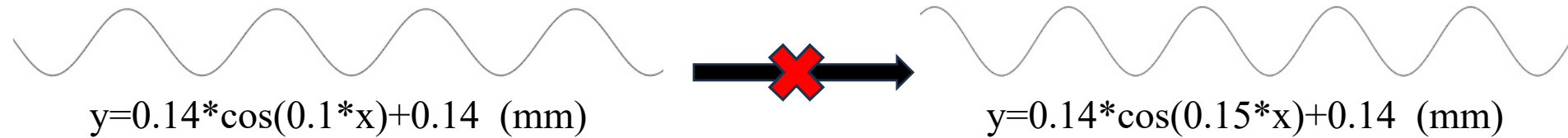
Illustration of training loss over epochs.



Results of predicted pressure under different fidelities.

Future work - 1

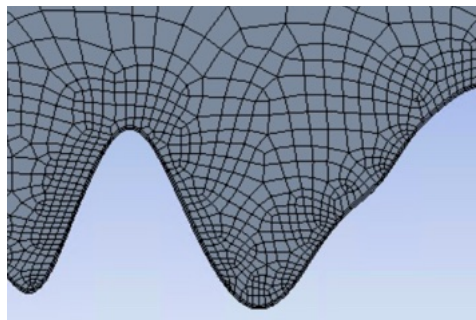
Task 2.1: Physics-guided inhibitor degradation prediction model



- Existing FNO framework cannot predict untrained roughness types
- Future work on enhancing the prediction power for extrapolation

Future work - 2

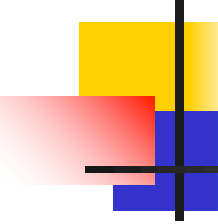
Upcoming works to include random roughness profile



$$\text{Chebyshev sampling: } V_{\text{poly}} = \left\{ \sum_{i=0}^{N-1} a_i T_i(x) : |a_i| \leq M \right\}$$

$$k_l(x_1, x_2) = \exp\left(-|x_1 - x_2|^2 / 2l^2\right) \longrightarrow \left| \frac{\partial^2 y}{\partial x^2} \right| < \delta$$

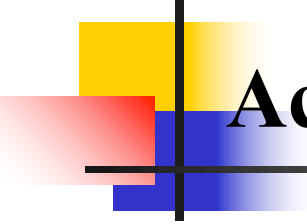
Illustration of the Gaussian smooth roughness shape as training data for more generalized prediction.

A decorative graphic on the left side of the slide consists of overlapping colored squares (yellow, red, blue) and a black crosshair.

Task 2: Simulation-based Inhibitor Implementation Optimization in Gas Gathering and Transportation Pipelines

Work plan for Q3

- Improve the applied numerical model to be more efficient by introducing local boundary condition near the roughness segment;
- Introduce random smoothing roughness models to improve the generalization of WSS prediction networks;
- Add turbulence, multiphase fluid into the existing pipe flow simulation, and consider more common pipe form, like the bending elbow.



Acknowledgments

This project is funded by DOT/PHMSA's Competitive Academic Agreement Program (Award No: 693JK32350004CAAP; Program Manager: Zhongquan Zhou & Nusnin Akter).

Please visit the below URL for more information:
<https://primis.phmsa.dot.gov/matrix/PrjHome.rdm?prj=506>

Task 2: Simulation-based Inhibitor Implementation Optimization in Gas Gathering and Transportation Pipelines

Task 2.1: Physics-guided inhibitor degradation prediction model

Initial Velocity	Pressure at Mid
0.50	-88.61
0.61	-68.37
0.72	-48.13
0.83	-27.89
0.94	-7.66
1.06	12.58
1.17	32.82
1.28	53.06
1.39	73.30
1.51	93.53

Low fidelity

Initial Velocity	Pressure at Mid
0.50	-1.00
1.00	-2.80
1.50	213.08

High fidelity

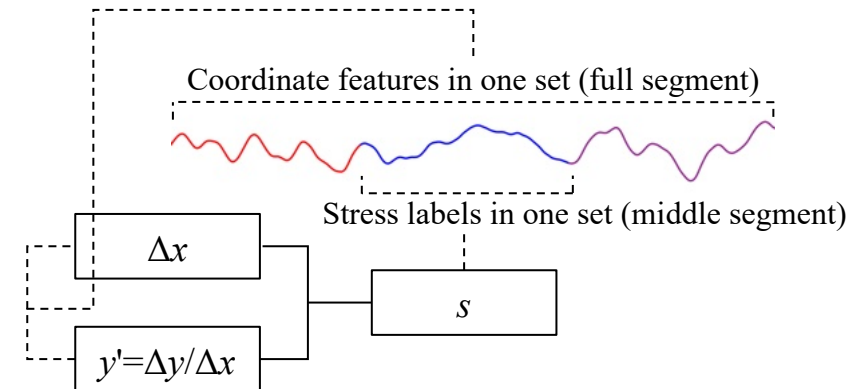
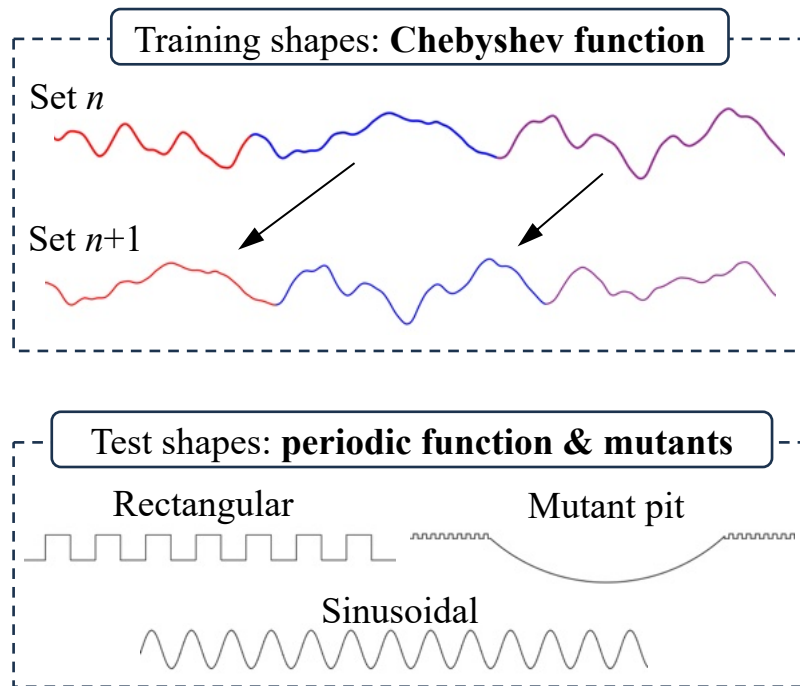
Initial Velocity	Pressure at Mid
0.65	-153.92
1.35	148.30

Validation high fidelity

Comparison between low fidelity and high Fidelity.

Future work - 1

Upcoming works to improve FNO



Input data: **increment** of grid node coordinates at flow direction (Δx) and roughness height direction ($y' = \Delta y / \Delta x$)

Output data: Wall shear stress (s) corresponding to the grid nodes

Illustration of data sampling considering near segments.